Guided Wave Optics

HENRY F. TAYLOR AND AMNON YARIV, FELLOW, IEEE

Invited Paper

Abstract—Phenomena associated with the propagation and manipulation of light in thin-film dielectric waveguides are presently the object of considerable research effort, directed toward possible applications in communications and information processing. The theory of dielectric waveguide modes is reviewed, and the topics of directional coupling, input-output coupling, modulation, and distributed feedback laser sources are treated on the basis of coupled-mode theory. A summary of experimental results for each of the guided-wave optical phenomena covered by the theory is also presented.

I. Introduction

THE TRANSMISSION and manipulation of optical power has long been the basis of a considerable industry as well as of substantial academic endeavor. The advent of the laser in 1960 stimulated a great deal of interest in the study of the properties of confined Gaussian beams which are emitted by laser oscillators. The spatial coherence of the laser field made it possible, for the first time, to obtain substantial powers in optical beams whose diffraction spread very nearly approaches the theoretical limit. The manipulation of these beams, by and large, was still accomplished by the "classical" prelaser means. Optical systems incorporating laser sources today are comprised essentially of the same components to be found in conventional optical systems. The laser radiation in the form of a propagating Gaussian beam passes in succession through discrete optical components which are individually secured to a common bed.

An alternative approach to the manipulation of radiation has long been used in the microwave portion of the spectrum. Here the guiding and processing of electromagnetic propagating beams is accomplished within low-loss (metallic) waveguides with cross-sectional dimensions comparable to the wavelength. These waveguides, which confine the radiation by repeated reflections from the walls, can propagate power at a given frequency in a number of spatially distinct modes with different phase (and group) velocities.

The possibility of applying the microwave approach to laser beams was suggested by the demonstration of discrete propagating modes in optical fibers by Snitzer and Osterberg [1] (1961) and by the demonstration by Yariv and Leite [2] and by Bond *et al.* [3] (1963) of planar dielectric waveguides in GaAs p-n junctions. A key experiment pointing the way to the control of such radiation was the modulation, by the electro-optic effect, of light guided by a p-n junction by Nelson and Reinhart [4] (1964). The rapid developments in the field of epitaxial thin films by Alferov *et al.* [5] (1969), Hayashi *et al.* [6] (1969), and Kressel and Nelson [7] (1969) led to the application of dielectric waveguiding principles in order to lower, dramatically, the threshold of GaAs injection lasers. Continuous room temperature operation was then possible, as demonstrated by Hayashi *et al.* [8] (1970). It also showed the way to a new family of dielectric waveguide devices based on epitaxy, as illustrated by Hall *et al.* [9] (1970).

The main theme of the developments in this field since 1969 was the demonstration of various guiding mechanisms and guided-wave phenomena. Here we may note the work on prism couplers by Tien *et al.* [10] (1969), and the work on grating couplers by Dakss *et al.* [11] (1970), which effectively provided solutions to the problem of coupling Gaussian laser beams into and out of dielectric waveguides. The concept of distributed feedback lasers, introduced by Kogelnik and Shank [12] (1971), seemed especially attractive as applied to lasers in guided-wave configurations, as illustrated by the corrugated epitaxial GaAs–GaAlAs lasers of Nakamura *et al.* [13] (1973).

The feasibility of optical directional coupling was illustrated by Somekh *et al.* [14] (1973) in power transfer experiments involving channel waveguides produced by ion implantation.

The use of the term "guided wave optics" in the title rather than "integrated optics" stems from our desire to distinguish between the investigation of optical phenomena in waveguides, the main topic here, and the integration of a number of optical components in a single structure in order to perform complex functions [15], [16], which we regard as the domain of integrated optics.

The purpose of the present paper is to review the main theoretical and experimental progress which has taken place in this field as well as to consider some of the more promising scientific and practical possibilities opened up by recent developments.

II. Waveguides and Waveguide Modes

A. Materials and Fabrication Techniques

A variety of materials and fabrication techniques have been used to make thin-film dielectric waveguides. Ion exchange in glass was one of the earliest methods reported [17]. Amorphous or polycrystalline film waveguides have been produced by vacuum deposition of ZnS [10] and Ta_2O_5 [18], and by sputtering of Ge [19]. Organic materials for waveguides have included polyester and polyurethane epoxy resins [20], vinyl trimethyl silane and hexamethyl disiloxane [21], cyclohexyl methacralate [22], polyphenyl siloxane [23], and polystyrene [24]. Films of nitrobenzene liquid [25] and of nematic liquid crystals [26], [27] have also exhibited waveguiding. Channel waveguides, which confine a beam in two dimensions, have been fabricated in sputtered glass films by sputter etching [28], [29], and in both fused silica [30] and

This invited paper is one of a series planned on topics of general interest—The Editor.

Manuscript received November 26, 1973; revised February 12, 1974. The work reported here was supported by Materials Sciences, Advanced Research Projects Agency, and by Aeronautics Programs, Office of Naval Research.

H. F. Taylor is with the Naval Electronics Laboratory Center, San Diego, Calif. 92152.

A. Yariv is with the Department of Electrical Engineering, California Institute of Technology, Pasadena, Calif. 91109.

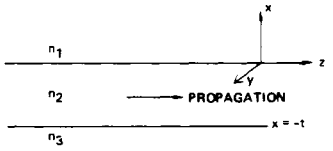

Fig. 1. A planar dielectric waveguide.

GaAs [14] by ion implantation. Solid-state diffusion has produced planar waveguides in $LiNbO_3$ [31] and channel waveguides in CdS [32], and ZnSe [33]. Waveguiding has been observed in planar epitaxial layers of GaAs [9], [34], GaAs-AlGaAs [35], Si [36], ZnSe [37], ZnO [38], and garnets [39]. Two-dimensional confinement has been demonstrated in mesa structures of epitaxial GaAs-AlGaAs [40], [41].

B. The Waveguide Modes [42], [43]

A prerequisite to an understanding of guided-wave interactions is a knowledge of the properties of the guided modes. A mode of a dielectric waveguide at a (radian) frequency ω is a solution of Maxwell's propagation equation

$$\nabla^2 E(r) + k^2 n^2(r) E(r) = 0 \tag{1}$$

subject to the continuity of the tangential components of E and H at the dielectric interfaces. In (1) the form of the field is taken as

$$E(r, t) = E(r) e^{i\omega t} \tag{2}$$

where $\omega \equiv kc$, and the index of refraction $n(r)$ is related to the dielectric constant $\epsilon(r)$ by $n^2(r) \equiv \epsilon(r)/\epsilon_0$. Limiting ourselves to waves with phase fronts normal to the waveguide axis z, we have

$$\left(\frac{\partial^2}{\partial x^2} + \frac{\partial^2}{\partial y^2}\right) E(x, y) + [k^2 n^2(r) - \beta^2] E(x, y) = 0. \tag{3}$$

The basic features of the behavior of dielectric waveguides can be extracted from a planar model in which no variation exists in one, say y, dimension. Channel waveguides, in which the waveguide dimensions are finite in both the x and the y directions, approach the behavior of the planar guide when one dimension is considerably larger than the other [44], [45]. Even when this is not the case, most of the phenomena discussed below are only modified in a simple quantitative way when going from a planar to a channel waveguide. Because of this and of the immense mathematical simplification which results, we will limit most of the treatment to planar waveguides such as the one shown in Fig. 1.

Putting $\partial/\partial y = 0$ in (3) and writing it separately for regions 1, 2, and 3 yields:

region 1

$$\frac{\partial^2}{\partial x^2} E(x, y) + (k^2 n_1^2 - \beta^2) E(x, y) = 0 \tag{4a}$$

region 2

$$\frac{\partial^2}{\partial x^2} E(x, y) + (k^2 n_2^2 - \beta^2) E(x, y) = 0 \tag{4b}$$

region 3

$$\frac{\partial^2}{\partial x^2} E(x, y) + (k^2 n_3^2 - \beta) E(x, y) = 0 \tag{4c}$$

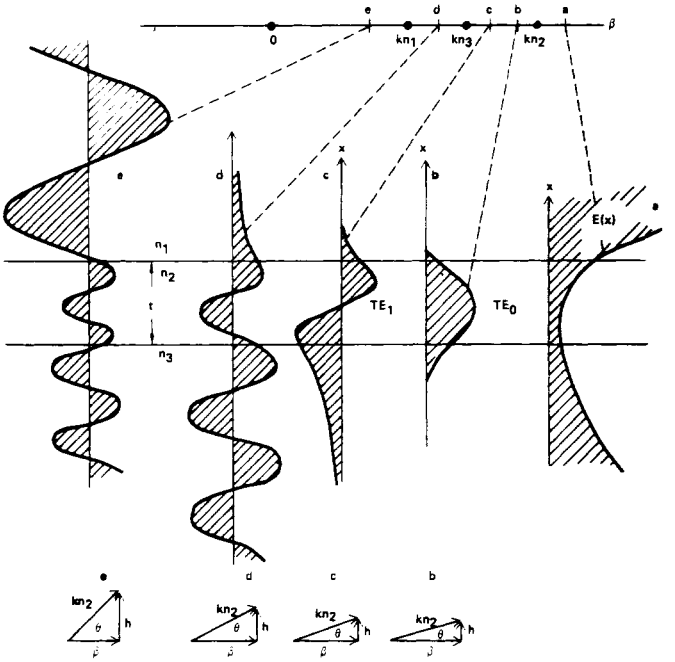

Fig. 2. Propagation constants, electric field distributions, and wave vector diagrams for the different types of waveguide modes: *a* is not physically realizable; *b* and *c* are guided modes; *d* is a substrate radiation mode; and *e* is a radiation mode of the waveguide.

where $E(x, y)$ is some Cartesian component of $E(x, y)$. Before embarking on a formal solution of (4) we may learn a great deal about the physical nature of the solutions by simple arguments. Let us consider the nature of the solutions as a function of the propagation constant β at some *fixed* frequency ω. Let us assume that $n_2 > n_3 > n_1$. For $\beta > kn_2$, i.e., region *a* in Fig. 2, it follows directly from (4) that

$$\frac{1}{E}\frac{\partial^2 E}{\partial x^2} > 0$$

everywhere and $E(x)$ is exponential in all three layers 1, 2, and 3 of the waveguides. Because of the need to match both $E(x)$ and its derivatives (see Section II-C) at the two interfaces, the resulting field distribution is as shown in Fig. 2(a). The field increases without bound away from the waveguide so that the solution is not *physically realizable* and thus does not correspond to a real wave.

For $kn_3 < \beta < kn_2$, as in points *b* and *c*, it follows from (4) that the solution is sinusoidal in region 2, since $(1/E)(\partial^2 E/\partial x^2) < 0$, but is exponential in regions 1 and 3. This makes it possible to have a solution $E(x)$ which satisfies the boundary conditions while *decaying* exponentially in regions 1 and 3. These solutions are shown in Fig. 2(b) and (c). The energy carried by these modes is confined to the vicinity of the guiding layer 2 and we shall, consequently, refer to them as confined or guided modes. From the foregoing discussion it follows that a necessary condition for their existence is that kn_1, $kn_3 < \beta < kn_2$ so that confined modes are possible only when $n_2 > n_1, n_3$, i.e., when the inner layer possesses the highest index of refraction.

Solutions of (4) for $kn_1 < \beta < kn_3$ (region *d*) correspond to exponential behavior in region 1 and to sinusoidal behavior in regions 2 and 3 as illustrated in Fig. 2(d). We shall refer to these modes as substrate radiation modes. For $0 < \beta < kn_1$, as in region *e*, the solution for $E(x)$ becomes sinusoidal in all

three regions. These are the so-called radiation modes of the waveguides.

A solution of (4), subject to the boundary conditions at the interfaces given in Section II-C, shows that while β can assume any value in regions d and e, the values of allowed β in the propagation regime $kn_3 < \beta < kn_2$ are discrete. The number of modes depends on the width t, the frequency, and the indices of refraction n_1, n_2, n_3. At a given wavelength, the number of guided modes increases from 0 with increasing t. At some t, the mode TE_0 becomes confined. Further increases in t will allow TE_1 to exist as well, and so on.

It is useful to view the wave in the inner layer 2 as a plane wave propagating at some angle θ to the horizontal axis and undergoing a series of total internal reflections at the interface 2–1 and 2–3. This is based on (4b). Assuming $E_x \propto \sin[hx + \alpha]$, we obtain

$$\beta^2 + h^2 = k^2 n_2^2. \tag{5}$$

The resulting right-angle triangles with sides β, h, and kn_2 are shown in Fig. 2. Note that since the frequency is constant, $kn_2 \equiv (\omega/c)\, n_2$ is the same for cases b, c, d, and e. The propagation can thus be considered formally as that of a plane wave along the direction of the hypotenuse with a propagation constant kn_2. As β decreases, θ increases until, at $\beta = kn_3$, the wave ceases to be totally internally reflected at the interface 3–2. The condition $\beta = kn_3$ is identified by writing $n_3 = n_2 \cos\theta$, which is the geometrical optics condition for the onset of total internal reflection.

C. Mode Characteristics of the Planar Waveguide

TE Modes: Consider the dielectric waveguide sketched in Fig. 1. It consists of a film of thickness t and index of refraction n_2 sandwiched between media with indices n_1 and n_3. Taking $\partial/\partial y = 0$, this guide can, in the general case, support a finite number of confined TE modes with field components E_y, H_x, and H_z and TM modes with components H_y, E_x, E_z. The "radiation" modes of this structure, which are not confined to the inner layer, are not treated here, but are important to the discussion of grating and prism couplers in Section V.

The field component E_y of the TE modes, as an example, obeys the wave equation

$$\nabla^2 E_y = \frac{n_i^2}{c^2}\frac{\partial^2 E_y}{\partial t^2}, \qquad i = 1, 2, 3. \tag{6}$$

We take $E_y(x, z, t)$ in the form

$$E_y(x, z, t) = \mathcal{E}_y(x) e^{i(\omega t - \beta z)}. \tag{7}$$

The transverse function $\mathcal{E}_y(x)$ is taken as

$$\mathcal{E}_y = \begin{cases} C\exp(-qx), & 0 \leqslant x < \infty \\ C[\cos(hx) - (q/h)\sin(hx)], & -t \leqslant x \leqslant 0 \\ C[\cos(ht) + (q/h)\sin(ht)]\exp[p(x+t)], & -\infty < x \leqslant -t \end{cases} \tag{8}$$

which, applying (6) to regions 1, 2, 3, yields

$$\begin{aligned} h &= (n_2^2 k^2 - \beta^2)^{1/2} \\ q &= (\beta^2 - n_1^2 k^2)^{1/2} \\ p &= (\beta^2 - n_3^2 k^2)^{1/2} \\ k &= \omega/c. \end{aligned} \tag{9}$$

From the requirement that E_y and H_z be continuous at $x = 0$ and $x = -t$, we obtain[1]

$$\tan(ht) = \frac{q + p}{h\left(1 - \frac{pq}{h^2}\right)}. \tag{10}$$

This equation in conjunction with (9) is used to obtain the eigenvalues β for the confined TE modes. An example of such a solution is shown in Fig. 3.

The constant C appearing in (8) is arbitrary, yet for many applications, especially those in which propagation and exchange of power involve more than one mode, it is advantageous to define C in such a way that total power is conserved. This point will become clear in Section III. We choose C so that the field $\mathcal{E}_y(x)$ in (8) corresponds to a power flow of *one* watt (per unit width in y direction) in the mode. A mode for which $E_y = A\mathcal{E}_y(x)$ will thus correspond to a power flow of $|A|^2$ W/m. The normalization condition becomes

$$-\frac{1}{2}\int_{-\infty}^{\infty} E_y H_x^* dx = \frac{\beta_m}{2\omega\mu}\int_{-\infty}^{\infty} [\mathcal{E}_y^{(m)}(x)]^2 dx = 1 \tag{11}$$

where the symbol m denotes the mth confined TE mode corresponding to the mth eigenvalue of (10).

Using (8) in (11) leads to

$$C_m = 2h_m\left[\frac{\omega\mu}{|\beta_m|\left(t + \frac{1}{q_m} + \frac{1}{p_m}\right)\left(h_m^2 + q_m^2\right)}\right]^{1/2}. \tag{12}$$

Since the modes $\mathcal{E}_y^{(l)}$ are orthogonal, we have

$$\int_{-\infty}^{\infty} \mathcal{E}_y^{(l)}\mathcal{E}_y^{(m)} dx = \frac{2\omega\mu}{\beta_m}\delta_{l,m}. \tag{13}$$

TM Modes: The field components are

$$\begin{aligned} H_y(x, z, t) &= \mathcal{H}_y(x) e^{i(\omega t - \beta z)} \\ E_x(x, z, t) &= \frac{i}{\omega\epsilon}\frac{\partial H_y}{\partial z} = \frac{\beta}{\omega\epsilon}\mathcal{H}_y(x) e^{i(\omega t - \beta z)} \\ E_z(x, z, t) &= -\frac{i}{\omega\epsilon}\frac{\partial H_y}{\partial x}. \end{aligned} \tag{14}$$

The transverse function $\mathcal{H}_y(x)$ is taken as

$$\mathcal{H}_y(x) = \begin{cases} -C\left[\frac{h}{q}\cos(ht) + \sin(ht)\right] e^{p(x+t)}, & x < -t \\ C\left[-\frac{h}{q}\cos(hx) + \sin(hx)\right], & -t < x < 0 \\ -\frac{h}{q} Ce^{-qx}, & x > 0. \end{cases} \tag{15}$$

The continuity of H_y and E_z at the two interfaces requires that the various propagation constants obey the eigenvalue

[1] The assumed form of $\mathcal{E}_y$ in (8) is such that $\mathcal{E}_y$ and $\mathcal{H}_z = (i/\omega\mu)\,\partial\mathcal{E}_y/\partial x$ are continuous at $x = 0$ and that $\mathcal{E}_y$ is continuous at $x = -t$. All that is left is to require continuity of $\partial\mathcal{E}_y/\partial x$ at $x = -t$. This leads to (10).

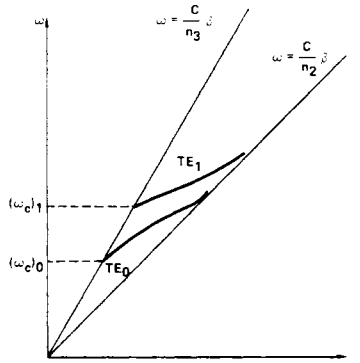

Fig. 3. Dispersion characteristic for TE_0 and TE_1 modes of planar waveguide, illustrating the cutoff frequencies $(\omega_c)_0$ and $(\omega_c)_1$.

equation

$$\tan(ht) = \frac{h(\bar{p}+\bar{q})}{h^2 - \bar{p}\bar{q}} \tag{16}$$

where

$$\bar{p} \equiv \frac{n_2^2}{n_3^2} p \qquad \bar{q} = \frac{n_2^2}{n_1^2} q.$$

The normalization constant C is chosen so that the field represented by (14) and (15) carries *one* watt per unit width in the y direction.

$$\frac{1}{2}\int_{-\infty}^{\infty} H_y E_x^* \, dx = \frac{\beta}{2\omega}\int_{-\infty}^{\infty} \frac{\mathcal{H}_y^2(x)}{\epsilon} dx = 1$$

or using $n_i^2 \equiv \epsilon_i/\epsilon_0$

$$\int_{-\infty}^{\infty} \frac{[\mathcal{H}_y^{(m)}(x)]^2}{n^2(x)} dx = \frac{2\omega\epsilon_0}{\beta_m}. \tag{17}$$

This condition determines the value of C_m as [46]

$$C_m = 2\sqrt{\frac{\omega\epsilon_0}{\beta_m t_{\text{eff}}}}$$

$$t_{\text{eff}} \equiv \frac{\bar{q}^2 + h^2}{\bar{q}^2}\left[\frac{t}{n_2^2} + \frac{q^2+h^2}{\bar{q}^2+h^2}\frac{1}{n_1^2 q} + \frac{p^2+h^2}{\bar{p}^2+h^2}\frac{1}{n_3^2 p}\right]. \tag{18}$$

III. Coupling Between Waveguide Modes

A. The Coupled-Mode Equations

Many of the experimental situations of guided wave optics and especially those which involve exchange of power between modes can be treated by means of the coupled-mode approach. This formalism, introduced originally by Pierce [47], describes the total propagating disturbance in a structure as a sum of (usually two) unperturbed modes of the system whose amplitudes vary with distance z due to some coupling between them. This point of view is fruitful when the z variation is slow, and has been applied to the description of different guided-wave phenomena [46]. In the following section we will reproduce some of the main features of this formalism.

Consider two electromagnetic modes with, in general, different frequencies whose complex amplitudes are A and B. These are taken as the eigenmodes of the unperturbed medium so that they represent propagating disturbances

$$a(z,t) = Ae^{i(\omega_a t - \beta_a z)} \qquad b(z,t) = Be^{i(\omega_b t \pm \beta_b z)} \tag{19}$$

where A and B are the complex normalized amplitudes which in the unperturbed structure are independent of z.

In the presence of a perturbation, power is exchanged between modes a and b. The complex amplitudes A and B in this case are no longer constant but will be found to depend on z. They will be shown to obey relations of the type

$$\frac{dA}{dz} = \kappa_{ab} B e^{-i\Delta z}$$

$$\frac{dB}{dz} = \kappa_{ba} A e^{+i\Delta z}. \tag{20}$$

The phase mismatch constant Δ merits some discussion. It is clear from the structure of (20) that a cumulative sustained exchange of power between modes a and b requires that $\Delta = 0$. Otherwise the values of dA/dz, for example, from different parts of the propagation path interfere destructively. In what follows we will find that in most of the problems of interest to us we can visualize the process of power exchange as follows. Traveling mode b interacts with the perturbation to yield a traveling polarization wave. This wave in turn drives mode a. Simultaneously, mode a interacts with the perturbation to drive mode b. The constant Δ is equal to the difference in the propagation constants of the driven waves and the driving polarizations.

The coupling coefficients κ_{ab} and κ_{ba} are determined by the physical situation under consideration and will be considered below.

Before proceeding with specific experimental situations we may draw some general conclusions which apply to the large number of phenomena which are described by equations of the general form of (20).

B. Codirectional Coupling

We take up, first, the case where modes a and b carry electromagnetic power in the *same* direction. It is extremely convenient to define, as was done in Section II, A and B in such a way that $|A(z)|^2$ and $|B(z)|^2$ correspond to the power carried by mode a and mode b, respectively. The conservation of total power is thus expressed as

$$\frac{d}{dz}(|A|^2 + |B|^2) = 0 \tag{21}$$

which, using (20), is satisfied when

$$\kappa_{ab} = -\kappa_{ba}^*. \tag{22}$$

If boundary conditions are such that a single mode, say b, is incident at $z = 0$ on the perturbed region $z > 0$, we have

$$b(0) \equiv B_0 \qquad a(0) = 0. \tag{23}$$

Subject to these conditions, the solutions of (20) become

$$A(z) = B_0 \frac{2\kappa_{ab}}{(4\kappa^2 + \Delta^2)^{1/2}} e^{-(i\Delta z/2)} \sin\left[\frac{1}{2}(4\kappa^2 + \Delta^2)^{1/2} z\right]$$

$$B(z) = B_0 e^{(i\Delta z/2)}\left\{\cos\left[\frac{1}{2}(4\kappa^2 + \Delta^2)^{1/2} z\right] - i\frac{\Delta}{(4\kappa^2+\Delta^2)^{1/2}}\sin\left[\frac{1}{2}(4\kappa^2+\Delta^2)^{1/2} z\right]\right\} \tag{24}$$

where $\kappa^2 \equiv |\kappa_{ab}|^2$.

Under phase-matched condition ($\Delta = 0$), a complete spatially periodic power transfer between modes a and b takes place with a period π/κ:

$$a(z, t) = B_0 \frac{\kappa_{ab}}{\kappa} e^{i(\omega_a t - \beta_a z)} \sin(\kappa z)$$

$$b(z, t) = B_0 e^{i(\omega_b t - \beta_b z)} \cos \kappa z. \tag{25}$$

A plot of the mode intensities $|a|^2$ and $|b|^2$ is shown in Fig. 4. This figure demonstrates the fact that for phase mismatch $|\Delta| >> |\kappa_{ab}|$ the power exchange between the modes is negligible. Specific physical situations which are describable in terms of this picture will be discussed further below.

C. Contradirectional Coupling

In this case the propagation in the unperturbed medium is described by

$$a = Ae^{i(\omega_a t + \beta_a z)}$$

$$b = Be^{i(\omega_b t - \beta_b z)} \tag{26}$$

where A and B are constant. Mode a corresponds to a left ($-z$) traveling wave while b travels to the right. A time–space periodic perturbation can lead to power exchange between the modes. Conservation of total power is now expressed as

$$\frac{d}{dz}(|A|^2 - |B|^2) = 0 \tag{27}$$

which is satisfied by (20) if we take

$$\kappa_{ab} = \kappa_{ba}^* \tag{28}$$

so that

$$\frac{dA}{dz} = \kappa_{ab} B e^{-i\Delta z} \qquad \frac{dB}{dz} = \kappa_{ab}^* A e^{i\Delta z}. \tag{29}$$

In this case we take the mode b with an amplitude B_0 to be incident at $z = 0$ on the perturbation region which occupies the space between $z = 0$ and $z = L$. Since mode a is generated by the perturbation we have $a(L) = 0$. With these boundary conditions, the solution of (29) is given by

$$A(z) = B_0 \frac{2i\kappa_{ab} e^{-i(\Delta z/2)}}{-\Delta \sinh \frac{SL}{2} + iS \cosh \frac{SL}{2}} \sinh\left[\frac{S}{2}(z - L)\right]$$

$$B(z) = B_0 \frac{e^{i(\Delta z/2)}}{-\Delta \sinh \frac{SL}{2} + iS \cosh \frac{SL}{2}} \left\{\Delta \sinh\left[\frac{S}{2}(z - L)\right] + iS \cosh\left[\frac{S}{2}(z - L)\right]\right\} \tag{30}$$

where

$$S \equiv \sqrt{4\kappa^2 - \Delta^2}, \quad \text{and} \quad \kappa \equiv |\kappa_{ab}|.$$

Under phase-matching conditions ($\Delta = 0$) we have

$$A(z) = B_0 \left(\frac{\kappa_{ab}}{\kappa}\right) \frac{\sinh[\kappa(z - L)]}{\cosh(\kappa L)}$$

$$B(z) = B_0 \frac{\cosh[\kappa(z - L)]}{\cosh(\kappa L)}. \tag{31}$$

A plot of the mode powers $|B(z)|^2$ and $|A(z)|^2$ for this case is shown in Fig. 5. For sufficiently large arguments of the cosh and sinh functions in (31), the incident mode power decays exponentially along the perturbation region. This decay, however, is due not to absorption but to reflection of power into the backward traveling mode a. This case will be considered in more detail in Section VII, where we discuss coupling by waveguide corrugations and distributed feedback lasers.

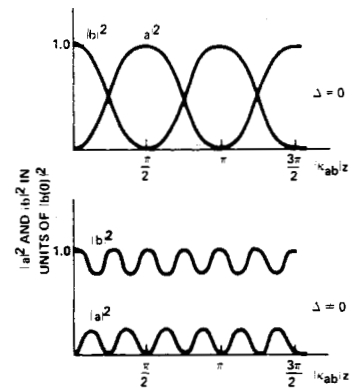

Fig. 4. Distribution of power between modes for codirectional coupling under phase-matched and unmatched conditions.

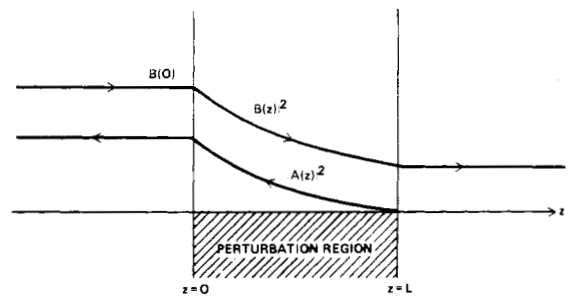

Fig. 5. Contradirectional transfer of power from an incident forward wave with amplitude $B(z)$ to a reflected wave $A(z)$.

D. The Coupling Coefficient

The general behavior of the two coupled modes is described by (24) and (30) for the case of codirectional and contradirectional coupling, respectively. The form of these equations is independent of the numerical magnitude of the coupling coefficient κ. The latter, however, determines the interaction strength or, in practice, the distance over which a given fractional power exchange between two modes takes place.

Consider coupling between, say, a TE mode

$$a^{(\pm)}(x, z, t) = A^{(\pm)}(z) e^{i(\omega_a t \mp \beta_a z)} \mathcal{E}_y^{(a)}(x) \tag{32}$$

and a forward-traveling TM mode

$$b^{+}(x, z, t) = B^{+}(z) e^{i(\omega_b t - \beta_b z)} \mathcal{H}_y^{(b)}(x) \tag{33}$$

where A and B are the power-normalized mode amplitudes. The (+) and (−) superscripts refer to forward and backward waves, respectively, and $\mathcal{E}_y(x)$ and $\mathcal{H}_y(x)$ are the normalized mode profiles as given by (8) and (15). The wave equation for the perturbed case is

$$\nabla^2 E_y(r, t) = \mu\epsilon \frac{\partial^2 E_y}{\partial t^2} + \mu \frac{\partial^2}{\partial t^2} [P_{\text{pert}}(r, t)]_y \tag{34}$$

where P_{pert} represents the deviation in the medium polarization

responsible for the mode coupling. Formal, but straightforward, considerations show that the coupling between the two modes is described by [46]

$$\frac{dA^{(-)}}{dz}e^{i(\omega_a t+\beta_a z)} - \frac{dA^{(+)}}{dz}e^{i(\omega_a t-\beta_a z)} = -\frac{i}{4\omega_a}\frac{\partial^2}{\partial t^2} \cdot \int_{-\infty}^{\infty} [P_{\text{pert}}(r,t)]_y \mathcal{E}_y^{(a)}(x)\,dx \quad (35)$$

where, in this case, $P_{\text{pert}}(r, t)$ is a polarization arising from the interaction of field of the TM mode, $b^+(x, z, t)$, and the medium perturbation responsible for the coupling of the two, otherwise independent, modes. This perturbation can be due, as an example, to a traveling sound wave, mechanical corrugations, an induced electrooptic birefringence, or magnetooptic Faraday rotation. Now synchronous exchange of power (i.e., one which does not fluctuate in time or space) requires that the exponents on both side of (35) be equal. Since this will not occur in general for both $A^{(-)}$ and $A^{(+)}$, coupling will take place from the forward TM mode to either $A^{(-)}$ or $A^{(+)}$. This last statement can be expressed analytically, by comparing (35) to (20), which gives

$$\kappa_{ab}^{(\pm)}e^{-i\Delta^{(\pm)}z} = \pm\frac{ie^{-i(\omega_a t\mp\beta_a z)}}{4\omega_a B^+}\frac{\partial^2}{\partial t^2} \cdot \int_{-\infty}^{\infty} [P_{\text{pert}}(r,t)]_y \mathcal{E}_y^{(a)}(x)\,dx. \quad (36)$$

In cases of interest to us $|\Delta^+| >> |\Delta^-|$ or vice versa, and coupling is limited to the pair of modes for which Δ is small. When we come to apply (36), as we will in the following sections, we find that $P_{\text{pert}}(r, t)$ is proportional to $B^+(z)e^{i\omega_a t}$ so that κ_{ab} is a constant.

E. Coupling by a Periodic Perturbation

Coupling of modes by a spatially periodic perturbation in refractive index is pertinent to a number of topics in guided wave optics, including grating couplers, directional couplers, distributed feedback lasers, and diffraction modulators. It will be assumed that the perturbation is periodic in the z direction. In the unperturbed case, the square of the refractive index is given by $n_0^2(x)$ and, in the perturbed case, by $n_0^2(x) + \Delta n^2(x, z)$. For coupling of two TE modes of a planar waveguide, the perturbation polarization is

$$[P_{\text{pert}}]_y = \epsilon_0 \Delta n^2 E_y \quad (37)$$

where E_y is given by

$$E_y = A\mathcal{E}_y^{(a)}(x)e^{i(\omega t-\beta_a z)} + B\mathcal{E}_y^{(b)}(x)e^{i(\omega t-\beta_b z)} \quad (38)$$

In the case of a sinusoidal surface ripple extending from $x = -a$ to $x = 0$, we have

$$\int_{-\infty}^{\infty}\Delta n^2\,dx = -\frac{a}{2}\left(n_2^2 - n_1^2\right)\left[1+\sin\left(\frac{2\pi z}{\Lambda}\right)\right] \quad (39)$$

where Λ is the period of the ripple, and n_1 and n_2 are the refractive indices on either side of the surface. The unperturbed surface is represented by the plane $x = 0$. Substituting this result into (36), and assuming that a is small, leads immediately to the result

$$|\kappa_{ab}| = \frac{\epsilon_0\omega}{16}\left(n_2^2 - n_1^2\right)a\left|\mathcal{E}_y^{(a)}\left(-\frac{a}{2}\right)\mathcal{E}_y^{(b)}\left(-\frac{a}{2}\right)\right| \quad (40)$$

for the magnitude of the coupling constant.

For a straight-walled corrugation of period Λ and depth a, the perturbation in refractive index can be written

$$\Delta n^2(x, z) = n_1^2 - n_2^2, \quad -a \leqslant x \leqslant 0, \quad N\Lambda < z < \left(N+\frac{1}{2}\right)\Lambda, \quad N = \text{integer}$$

$$\Delta n^2(x, z) = 0 \text{ elsewhere.} \quad (41)$$

This index variation in the region $-a \leqslant x \leqslant 0$ can be expanded in the series

$$\Delta n^2 = (n_1^2 - n_2^2)\left[\frac{1}{2}+\frac{2}{\pi}\left(\sin\frac{2\pi z}{\Lambda}+\frac{1}{3}\sin\frac{3\cdot 2\pi z}{\Lambda} + \cdots + \frac{1}{l}\sin\frac{l\cdot 2\pi z}{\Lambda}\right)\right] \quad (42)$$

and it is easily shown that

$$|\kappa_{ab}^{(l)}| = \frac{\epsilon_0\omega}{4\pi l}(n_2^2 - n_1^2)a\left|\mathcal{E}_y^{(a)}\left(-\frac{a}{2}\right)\mathcal{E}_y^{(b)}\left(-\frac{a}{2}\right)\right| \quad (43)$$

where l is the order of the harmonic responsible for coupling. For the special case of contradirectional coupling involving the nth guided TE mode of a planar (slab) waveguide, it can be shown that

$$|\kappa_{ab}^{(l)}| = \frac{\lambda a n^2}{2t^3 n_2 l} \quad (44)$$

in the limit of small a, where t is the waveguide thickness and λ is the free-space wavelength. It is assumed that the mode is strongly guided. This expression is referred to in the treatment of distributed feedback lasers (Section VII).

Another case of interest is that in which the perturbation is uniform in the x direction. For a sinusoidal index variation in the y direction, of infinite extent, the index variation is

$$\Delta n^2 = q\sin\left(\frac{2\pi y}{\Lambda}\right) \quad (45)$$

where q is the amplitude of the perturbation. Substituting this into (37) and combining with (36) yields

$$|\kappa_{ab}| = \frac{\epsilon_0\omega q}{8}\left|\int_{-\infty}^{\infty}\mathcal{E}_y^{(a)}(x)^*\,\mathcal{E}_y^{(b)}(x)\,dx\right|. \quad (46)$$

Because of the orthogonality condition (13), coupling in this case will occur only between modes of the same order, that is, only if $\mathcal{E}_y^{(a)}(x) = \mathcal{E}_y^{(b)}(x)$. Evaluation of (46) yields

$$|\kappa_{ab}| = \frac{\epsilon_0\omega^2\mu q}{4\beta_a}. \quad (47)$$

The propagation vectors β_a and β_b for the coupled modes will be equal in magnitude, but have a different angular orientation in the y-z plane, as determined by the condition that the waves be synchronous in the y direction: $(\beta_a)_y = (\beta_b)_y \pm (2\pi/\Lambda)$. This point will be developed further in Section VI.

The coupling between two modes with propagation vectors β_a and β_b will be strongest if the phase-match condition $\Delta = 0$ is satisfied, where

$$\Delta = (\beta_a)_z - (\beta_b)_z \pm \left(\frac{2\pi l}{\Lambda}\right) \quad (48)$$

for lth-order coupling ($l = 1$ for a sinusoidal perturbation). Codirectional coupling will occur if $(\beta_a)_z$ and $(\beta_b)_z$ have the

same sign, and contradirectional coupling, if these quantities are of opposite sign. Solutions to the coupled-mode equations for these two cases are given by (24) and (30), respectively.

IV. Directional Coupling

Exchange of power between guided modes of parallel waveguides is known as directional coupling. It is anticipated that waveguide directional couplers will perform a number of useful functions in thin-film devices, including power division, modulation, switching, frequency selection, and polarization selection.

If two coupled waveguides have equal propagation constants (synchronous case), complete transfer of power from one waveguide to the other is possible; if the propagation constants are unequal (asynchronous case), only a fraction of the power initially propagating in one waveguide can be transferred to the other. Theoretical treatments of both synchronous [43], [44], [48] and asynchronous [49], [50] cases have been given. Experimentally, coupling has been observed between glass fibers [51], between planar films of glass [52], between channel waveguides in glass [29], and in GaAs [14], [53].

Waveguide coupling can be treated theoretically by coupled-mode theory. Consider the case of the two planar waveguides illustrated in Fig. 6. Refractive index distributions for the two guides in the absence of coupling are given by $n_a(x)$ and $n_b(x)$. The transverse electric field distribution for a particular guided mode of waveguide a and a particular mode of waveguide b will be denoted by $\mathcal{E}_y^{(a)}$ and $\mathcal{E}_y^{(b)}$, and the propagation constants by β_a and β_b. The field for the coupled-guide structure for propagation in the positive z direction is approximated by

$$E_y = A(z)\,\mathcal{E}_y^{(a)}(x)\,e^{i(\omega t-\beta_a z)} + B(z)\,\mathcal{E}_y^{(b)}(x)\,e^{i(\omega t-\beta_b z)}. \quad (49)$$

The perturbation polarization responsible for the coupling is calculated by substituting (49) into (34), neglecting the variation of A and B. The result is

$$P_{\text{pert}} = -e^{i\omega t}\epsilon_0\left[\mathcal{E}_y^{(a)}A(z)\left(n_c^2 - n_a^2\right)e^{-i\beta_a z} + \mathcal{E}_y^{(b)}B(z)\left(n_c^2 - n_b^2\right)e^{-i\beta_b z}\right] \quad (50)$$

where $n_c(x)$ is the refractive index for the two-guide structure.

Substituting (50) into (35) and integrating over x yields

$$\frac{dA}{dz} = \kappa_{ab}Be^{-i\Delta z} + M_a A$$

$$\frac{dB}{dz} = \kappa_{ab}Ae^{i\Delta z} + M_b B \quad (51)$$

where

$$\Delta = \beta_a - \beta_b$$

$$\kappa_{ab} = -\frac{i\epsilon_0\omega}{4}\int_{-\infty}^{\infty}\left(n_c^2 - n_a^2\right)\mathcal{E}_y^{(a)}\mathcal{E}_y^{(b)}\,dx$$

$$M_{(a,b)} = -\frac{i\epsilon_0\omega}{4}\int_{-\infty}^{\infty}\left(n_c^2 - n_{(a,b)}^2\right)\left(\mathcal{E}_y^{(a,b)}\right)^2\,dx. \quad (52)$$

The terms M_a and M_b represent small corrections to β_a and β_b, so (51) reduces to the familiar form (20), with $\Delta = \beta_a - \beta_b - i(M_a - M_b)$. The solution is given by (24). If a power P_0 is initially coupled into guide b at $z = 0$, the interguide

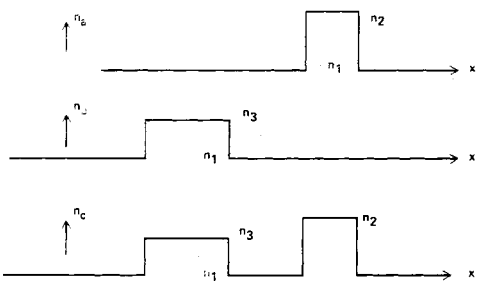

Fig. 6. Spatial variation of refractive index for uncoupled waveguides $n_a(x)$ and $n_b(x)$, and for a parallel waveguide structure $n_c(x)$.

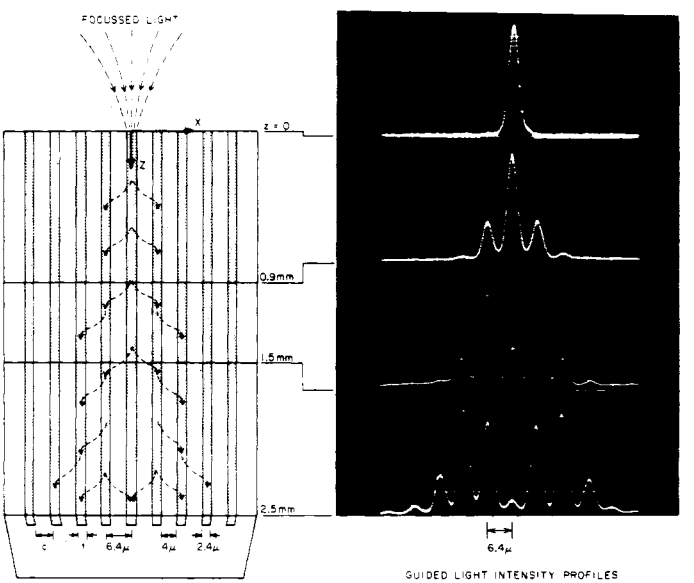

Fig. 7. Experimental results demonstrating directional coupling in GaAs waveguides.

distribution for $z > 0$ is given by

$$P_a = P_0\frac{4\kappa^2}{4\kappa^2 + \Delta^2}\sin^2\left[\frac{(4\kappa^2 + \Delta^2)^{1/2}z}{2}\right]$$

$$P_b = P_0\left\{\frac{\Delta^2}{4\kappa^2 + \Delta^2} + \frac{4\kappa^2}{4\kappa^2 + \Delta^2}\cos^2\left[\frac{(4\kappa^2 + \Delta^2)^{1/2}z}{2}\right]\right\}. \quad (53)$$

Complete power transfer occurs in a distance $L = \pi/2\kappa$ in the synchronous case ($\Delta = 0$). In the asynchronous case ($\Delta \neq 0$), both coupling length and maximum power transfer are less than in the synchronous case.

Coupling between waveguides with different propagation constants ($\beta^{(a)} \neq \beta^{(b)}$) can be improved by a periodic perturbation in refractive index. Most efficient coupling by a sinusoidal perturbation requires that $\Delta = 0$, where

$$\Delta = \beta_a \pm \beta_b \pm \frac{2\pi}{\Lambda} \quad (54)$$

and Λ is the period of the perturbation, measured in the z direction. Both codirectional and contradirectional power transfer are possible [54].

The preceding discussion assumes that only two waveguides are involved in the coupling, but coupled-mode theory can also be applied to problems involving more than two waveguides. In the case of an array of equally spaced, synchronous

waveguides, the coupled-mode relations are

$$\frac{dA_n}{dz} = \kappa(A_{n-1} + A_{n+1}) \tag{55}$$

where κ is given by (52), and A_n represents the mode amplitude for the nth waveguide. If all of the incident power is initially in the zeroth guide for $z = 0$, the solution to (55) is

$$A_n(z) = A_0(0)\,(-i)^n J_n(2i\kappa z) \tag{56}$$

for $z > 0$ [14], where J_n is the Bessel function of order n. Experimental results illustrating this behavior are given in Fig. 7.

V. Input-Output Coupling

Efficient coupling of light into and out of a thin film is an important consideration in guided wave optics experiments and devices. Three commonly used coupling techniques are illustrated in Fig. 8. Efficient coupling by the "end-fire" technique [Fig. 8(a)] requires that the exposed waveguide surface be smooth, in order to avoid excessive scattering of the incident beam. Good optical surfaces at the edge of the film can usually be obtained only by cleaving a crystal. With the prism coupler [10], [20], [55] [Fig. 8(b)], light enters through the top surface of the film, which can generally be made very smooth. In this type of coupler, a narrow (e.g., 1000 Å) gap of air or other low-refractive-index material separates the prism from the film. Optical power enters or leaves the film by tunneling through the gap. For most efficient power transfer, the phase velocity of the light wave in the prism must match that of a guided mode of the waveguide. Mathematically, this condition can be written as follows

$$\left(\frac{2\pi}{\lambda}\right) n_p \sin\theta = \beta_n \tag{57}$$

where λ is the free-space wavelength, n_p is the refractive index of the prism, θ is the angle between the incident beam in the prism and the normal to the surface of the film, and β_n is the propagation constant of a particular mode in the film. By varying θ, different modes of the film can be excited; in output coupling, different modes are identified by the angles at which they emerge from the film. Input coupling efficiencies of 88 percent have been reported [56].

A phase grating deposited on the surface of the film [Fig. 8(c)] can also provide efficient coupling [11], [57]-[60]. In this case, the phase-match condition is

$$\left(\frac{2\pi}{\lambda}\right) n_1 \sin\theta \pm \frac{2l\pi}{\Lambda} = \beta_n \tag{58}$$

where n_1 is the refractive index of the air or other medium in which the incident beam propagates, Λ is the grating period, and l is the diffraction order of the grating (an integer). Light is coupled either through the top surface of the film, as illustrated, or through the substrate. Both codirectional and contradirectional coupling have been demonstrated. Once again, angular differences in input and output beams correspond to different waveguide modes. Input efficiencies as high as 71 percent have been observed [61], [62].

A fourth type of coupler, not illustrated, makes use of the tapered edges of the film itself for deflecting an incident beam into, or a transmitted beam out of, the film [63]. Efficiencies of 40 percent have been reported for input coupling.

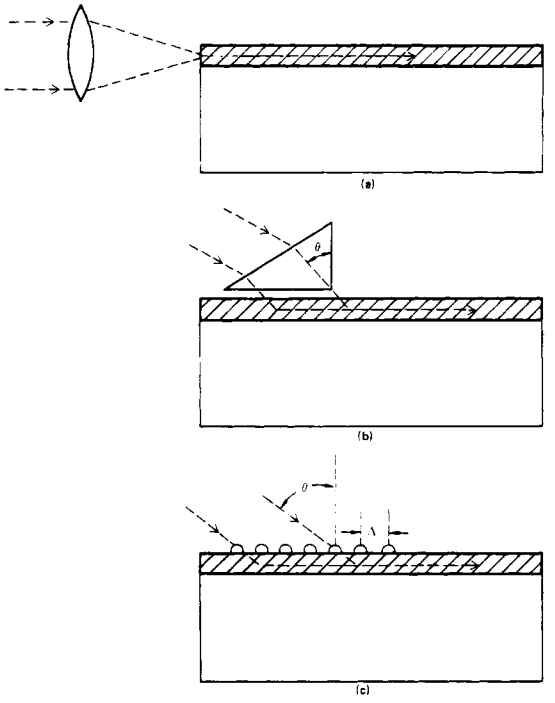

Fig. 8. Techniques for coupling light into a thin-film waveguide. (a) Endfire. (b) Prism coupler. (c) Grating coupler.

A feature which is common to both prism and grating couplers is that, in both, power is exchanged between a guided mode and a continuum of modes. In the grating coupler, the continuum consists of the radiation modes of the waveguide itself. In the prism coupler, the continuum modes comprise the angular spectrum of plane waves which can propagate in the uniform material of the prism. Equations which describe coupling from one mode to a continuum are

$$\frac{dA_\beta}{dz} = \kappa_{\beta_0\beta}\, e^{i(\beta-\beta_0)z} B$$

$$\frac{dB}{dz} = \pm \int \kappa^*_{\beta_0\beta}\, \sigma_\beta A_\beta\, e^{-i(\beta-\beta_0)z}\, d\beta \tag{59}$$

where $\kappa_{\beta_0\beta}$ is the coupling constant, A_β and B are the respective mode amplitudes for continuum and guided modes, β and β_0 are the propagation constants, and σ_β is the mode density (number of modes per unit β) for the continuum. The plus and minus signs in the second equation refer, respectively, to contradirectional and codirectional coupling. The expression (59) is simply a generalization of (20), which describes coupling between two modes.

Since the interaction in the case of the grating coupler involves modes of the same waveguide, the calculation of the coefficients $\kappa_{\beta_0\beta}$ follows the treatment of mode coupling by a surface corrugation, given in Section III-E. The prism coupler, on the other hand, can be thought of as two parallel waveguides, in which one of the "waveguides" (the prism itself) is of infinite extent and will thus support a continuum of guided modes. In either case, if the incident wave travels in a medium of refractive index n_0, the mode fields in that medium will have the form

$$E_y \alpha \sin(\gamma_\beta x + \phi_\beta) \tag{60}$$

where

$$\gamma_\beta^2 + \beta^2 = \left(\frac{2\pi n_0}{\lambda}\right)^2 \tag{61}$$

and ϕ_β is determined by the boundary conditions. The mode density in γ_β space is constant, and it follows from (61) that $\sigma_\beta \propto 1/\gamma_\beta$.

We consider first the output coupling problem; all of the power is in the guided mode at $z = 0$ and propagates in the positive z direction. The boundary conditions are $B(0) = B_0$, and $A_\beta(0) = 0$, all β, for the codirectional case; and $B(0) = B_0$, $A_\beta(L) = 0$, all β, for the contradirectional case, where L is the length of the coupler. If $\kappa_{\beta_0\beta}$ and σ_β are independent of β, the solution to (59) for B is

$$B = B_0 e^{-\alpha z} \tag{62}$$

with

$$\alpha = \pi \left|\kappa_{\beta_0\beta}\right|^2 \sigma_\beta \tag{63}$$

in both cases. The solution for A_β is

$$A_\beta = \kappa_{\beta_0\beta} B_0 \left[\frac{e^{[i(\beta-\beta_0)-\alpha]z} - 1}{i(\beta - \beta_0) - \alpha}\right] z \geqslant 0 \tag{64}$$

for the codirectional coupling, and

$$A_\beta = \kappa_{\beta_0\beta} B_0 \left\{\frac{e^{[i(\beta-\beta_0)-\alpha]z} - e^{[i(\beta-\beta_0)-\alpha]L}}{i(\beta - \beta_0) - \alpha}\right\} 0 \leqslant z \leqslant L \tag{65}$$

for contradirectional coupling.

Input coupling efficiency can be computed by using the results just obtained for the reciprocal problem of output coupling [64]. We recall that the field distribution for the output coupling problem is given by

$$[E_y]_{\text{out}} = B \mathcal{E}_y^{(0)} e^{i(\omega t - \beta_0 z)} + \int \sigma_\beta A_\beta e^{i(\omega t - \beta z)} \mathcal{E}_y^{(\beta)} d\beta. \tag{66}$$

If the field of an input beam is $[E_y]_{\text{in}}$, then the coupling efficiency η is

$$\eta = \frac{\left|\int_{-\infty}^{\infty} [E_y]_{\text{out}}^* [E_y]_{\text{in}} dx\right|^2}{\int_{-\infty}^{\infty} \left|[E_y]_{\text{in}}\right|^2 dx \int_{-\infty}^{\infty} \left|[E_y]_{\text{out}}\right|^2 dx} \tag{67}$$

where the integrands are evaluated at a particular value of z. The input coupling efficiency is thus determined by how well the field of input beam matches the radiation pattern for an output beam. The maximum coupling efficiency is found to be 81 percent for a plane-wave input if the coupling strength $\kappa_{\beta_0\beta}$ is independent of z [65], [66]. In the case of a prism coupler with a linearly tapered gap, theory predicts a coupling efficiency of 96 percent [56].

The preceding arguments are valid for the grating coupler if only one set of guided modes, corresponding to one grating order, is involved in the coupling. If coupling to other grating orders is significant, the efficiency for input coupling is reduced. These undesired orders have been effectively suppressed or eliminated in experimental devices by using a thick "Bragg" grating [61] and by employing a grating with a short period for contradirectional coupling to substrate radiation modes [62].

VI. Modulation

Thin-film optical waveguide modulators may find widespread application in communications and information processing systems because of their high bandwidth, low electrical power requirements, and compatibility with other thin-film components. These devices consist of a dielectric waveguide and an appropriate electrode structure. An applied electric or magnetic field or an acoustic wave alters the dielectric tensor of the material in such a manner as to change the amplitude, phase, or frequency of the guided light wave. Materials used to date have included semiconducting III-V and II-VI compounds, $LiNbO_3$, and nitrobenzene liquid for electrooptic devices, garnets for magnetooptic devices, and glass films on quartz and $LiNbO_3$ substrates for acoustooptic devices. This section will consider the theory, fabrication, and performance of the various types of waveguide modulator.

A. The Dielectric Tensor

The elements of the dielectric tensor $\tilde{\epsilon}$ satisfy the relation

$$\sum_i \frac{x_i^2}{\epsilon_i} + \sum_{i \neq j} \frac{\epsilon_{ij} x_i x_j}{\epsilon_i \epsilon_j} = \frac{1}{\epsilon_0} \tag{68}$$

where $i, j = 1, 2, 3$, the x_i's are Cartesian coordinates, and ϵ_0 is the permittivity of free space. In discussing bulk modulators, it is convenient to choose the principal coordinate system such that $\tilde{\epsilon}$ is diagonal in the absence of the interaction. An element of $\tilde{\epsilon}$ is written

$$\epsilon_{ij} = \epsilon_i^{(0)} \delta_{ij} + \Delta\epsilon_{ij} \tag{69}$$

where $\epsilon_i^{(0)}$ is the diagonal element in the unperturbed case, and $\Delta\epsilon_{ij}$ is the induced change. A change in the dielectric tensor induced by an applied electric field E is expressed in terms of the elements of the electrooptic tensor r_{ijk} as

$$\Delta\epsilon_{ij} = \sum_k \frac{\epsilon_i \epsilon_j}{\epsilon_0} r_{ijk} E_k.$$

In the acoustooptic case, the corresponding relation is

$$\Delta\epsilon_{ij} = \sum_{kl} \frac{\epsilon_i \epsilon_j P_{ijkl} S_{kl}}{\epsilon_0} \tag{70}$$

where P_{ijkl} is the photoelastic tensor element and S_{kl} is an element of the strain field of the sound wave. In the magnetooptic case, with the modulating field directed along the z axis, the dielectric tensor has the form

$$\tilde{\epsilon} = \begin{vmatrix} \epsilon_x & -i\delta & 0 \\ i\delta & \epsilon_y & 0 \\ 0 & 0 & \epsilon_z \end{vmatrix} \tag{71}$$

where the off-diagonal elements $\pm i\delta$ are induced by the applied field.

In discussing modulation in waveguides, it is usually convenient to use coordinates $\{x_i'\}$ appropriate to the geometry of the waveguide, which may not correspond to the principal coordinates of the bulk crystal. The relation (68) can be used to transform the dielectric tensor from one set of coordinates to the other. Finally, it is evident from (34) that the relation between an induced change in the dielectric tensor and a

component of polarization of the medium is simply

$$[P_{\text{pert}}]_i = \sum_j \Delta\epsilon_{ij} E_j. \tag{72}$$

This relation will be used in calculating the behavior of the various types of modulator.

B. Waveguide Modulation

Thin-film modulators can be classified according to the manner in which a change in the dielectric tensor $\Delta\epsilon_{ij}$ affects the propagation of power in waveguide modes. For example, a phase grating set up in the medium by an electrooptic or acoustooptic interaction can diffract a guided light beam. In the following discussion, the devices which have been demonstrated or proposed are divided into these categories: 1) relative phase control, 2) polarization rotation, 3) grating diffraction, 4) waveguide cutoff, 5) interguide coupling, and 6) attenuation.

In the *relative phase* modulator, the phase of guided modes of one polarization is changed with respect to that of modes of orthogonal polarization. The phase change results from a perturbation which affects the expectation values, in some coordinate system, of diagonal elements of the dielectric tensor. No coupling between modes is involved. For example, the differential equation of the amplitude of the mth TE mode of a planar waveguide is, from (35) and (72),

$$\frac{dA_m}{dz} = \frac{-i\omega}{4} \langle \Delta\epsilon_y \rangle_{mm} A_m \tag{73}$$

where

$$\langle \Delta\epsilon_{ij} \rangle_{mn} = \int_{-\infty}^{\infty} \Delta\epsilon_{ij} \mathcal{E}_i^{(m)*} \mathcal{E}_j^{(n)} \, dx. \tag{74}$$

The solution to (73) is

$$A_m(z) = A_m(0) \, e^{-i\omega \langle \Delta\epsilon_y \rangle_{mm} z/4}. \tag{75}$$

The relative phase difference $\Delta\phi$ between TE and TM modes which are in phase at $z = 0$ is thus

$$\Delta\phi = \left[\beta_{\text{TM}} - \beta_{\text{TE}} + \frac{\omega}{4} (\langle \Delta\epsilon_x \rangle_{mm} - \langle \Delta\epsilon_y \rangle_{mm}) \right] z \tag{76}$$

where β_{TE} and β_{TM} are propagation constants in the absence of the perturbation. For spatially uniform changes in the dielectric tensor,

$$\langle \epsilon_x \rangle_{mm} \sim \frac{2\omega\mu\epsilon_0 n_x^2}{\beta_m}$$

so that

$$\omega \langle \Delta\epsilon_x \rangle_{mm} \sim \frac{4\omega^2 \mu\epsilon_0 n_x \Delta n_x}{\beta_m} \sim \frac{8\pi \Delta n_x}{\lambda}.$$

Then (76) reduces to the more familiar result

$$\Delta\phi = \left[\beta_{\text{TM}} - \beta_{\text{TE}} + \left(\frac{2\pi}{\lambda} \right) (\Delta n_x - \Delta n_y) \right] z.$$

Bulk electrooptic modulators [67] are relative phase devices, and the same principle has been used in the thin-film configuration. Fig. 9(a) is a schematic illustration of such a device. A linearly polarized light beam is coupled into a waveguide in which the relative phase of orthogonal polarization components is controlled by an applied electric field. The phase-modulated output from the waveguide becomes intensity-modulated upon passing through an analyzer, which transmits only a selected polarization component. If the polarization of the output beam is oriented at 45° to the principal axes, and the analyzer is set to pass light with the same polarization as the input beam, the intensity I of the modulated output is

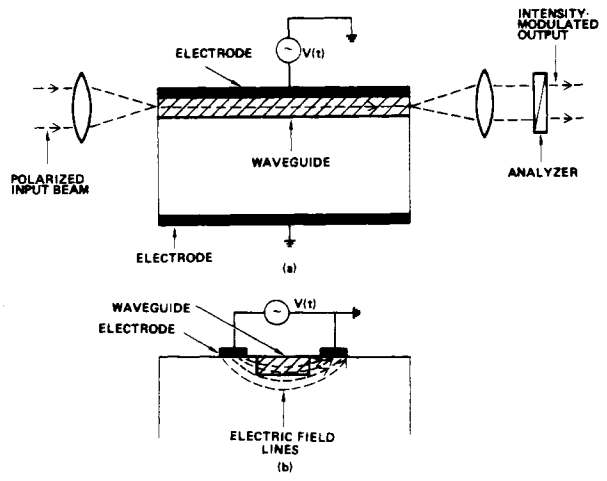

Fig. 9. Two configurations for relative-phase electrooptic modulator. (a) Planar waveguide. (b) Channel waveguide.

$$I = I_m \cos^2 \frac{\Delta\phi}{2} \tag{77}$$

where I_m is the maximum intensity. An induced relative-phase change of $\pm\pi$ radians is required for 90° rotation in polarization, giving rise to complete intensity modulation. For intermediate values of the phase change, the light emerging from the waveguide will be elliptically polarized. The phase difference is proportional to the interaction length and, in the linear electrooptic crystals generally used for these devices, to the applied electric field.

Waveguide electrooptic modulation was first observed a decade ago in diffusion-doped GaP diodes [4], and subsequent efforts have improved the performance and understanding of these devices [68], [69]. Waveguiding confines the light to the high-field region in the vicinity of the reverse-biased p-n junction. Relative-phase modulation has also been observed in epitaxial layers of GaAs in a Schottky barrier configuration [9]. Best results to date for a planar structure were obtained in a reverse-biased GaAs–$Al_x Ga_{1-x}$As double-heterostructure diode grown by liquid epitaxy [70]. Only 10 V were required for a π-radian relative-phase shift in a 1-mm-long device. Recently, modulation in planar waveguides produced by out-diffusion of Li from $LiNbO_3$ substrates has been reported [71]. The modulating voltage was applied to parallel stripe electrodes deposited on the waveguide surface. In another device, illustrated in Fig. 9(b), channel waveguides which provided beam confinement in two dimensions were fabricated by masked diffusion of Se into CdS and Cd into ZnSe [72].

In the *polarization rotation* modulator, power is exchanged between modes of orthogonal polarization, which are coupled via the off-diagonal elements of the dielectric tensor. We

consider coupling between the mth TE mode and the nth TM mode of a waveguide, with respective amplitudes A_m and B_n. The coupled-mode equations, obtained from (35) and (72), are

$$\frac{dA_m}{dz} = \frac{-i\omega}{4} e^{i(\beta_{TE}^{(m)} - \beta_{TM}^{(n)})z} \langle \Delta\epsilon_{yx} \rangle_{nm} B_n$$

$$\frac{dB_n}{dz} = \frac{-i\omega}{4} e^{-i(\beta_{TE}^{(m)} - \beta_{TM}^{(n)})z} \langle \Delta\epsilon_{xy} \rangle_{mn} A_m. \quad (78)$$

These relations have the form (20), and the solution for codirectional coupling is given by (24), with

$$\kappa = \frac{-i\mu\omega^2}{4} \langle \Delta\epsilon_{yx} \rangle_{nm}$$

and

$$\Delta = \beta_{TE}^{(m)} - \beta_{TM}^{(n)}.$$

Coupling between TE and TM modes is efficient only if β_{TE} and β_{TM} are nearly equal. In particular, if $\Delta = 0$ and $A_m(0) = 0$, we have from (25)

$$A_m(z) = B_n(0) \frac{\kappa}{|\kappa|} \sin |\kappa| z$$

$$B_n(z) = B_n(0) \cos |\kappa| z. \quad (79)$$

If κ is real, as will be the case in magnetooptic modulation ($\Delta\epsilon_{xy}$ imaginary), the polarization of a linearly polarized incident beam will rotate as a function of propagation distance. If κ is imaginary ($\Delta\epsilon_{xy}$ real), the modulation is of the relative-phase type with reference to axes oriented at 45° to the x and y axes. Thus electrooptic coupling, even by off-diagonal elements of $\tilde{\epsilon}$, is of the relative-phase type.

In bulk magnetooptic devices, a modulating field applied in the direction of optical propagation causes a rotation in the polarization vector of the beam. The same principle has been used to obtain modulation in an epitaxial iron–garnet film on a gadolinium–garnet substrate [73]. However, in the thin-film device it was necessary to employ the electrode structure illustrated in Fig. 10 to achieve phase-matching between TE and TM modes of the waveguide. Current in the electrodes sets up a magnetic field with spatial period Λ. The phase-match condition becomes

$$\beta_{TE} \pm \frac{2\pi l}{\Lambda} = \beta_{TM}$$

with l an integer corresponding to the diffraction order. Over 50 percent of the power coupled into a TM mode was converted to TE modes in the experimental device. The use of a highly birefrigent prism for output coupling provided for wide angular separation of the two polarization components.

The polarization of an optical guided wave can be altered by a shear acoustic wave which is polarized normal to the direction of optical propagation. Conversion between TE and TM modes has been produced by bulk acoustic waves in glass and in polyurethane waveguides [74], [75].

In the *spatial diffraction modulator*, a light beam is deflected by a periodic perturbation in refractive index (phase grating). The perturbation can be produced by an electrooptic, magnetooptic, or acoustooptic interaction. An important property of this grating is its momentum vector k_g, which is directed normal to and coplanar with the rulings and is equal in magnitude to $2\pi/\Lambda$, where Λ is the grating period. For the planar geometry of previous examples, we have two phase-match conditions:

$$(\beta_i)_y \pm l(k_g)_y = (\beta_d)_y \quad (80)$$

and

$$(\beta_i)_z \pm l(k_g)_z = (\beta_d)_z \quad (81)$$

where β_i and β_d are propagation vectors for incident and diffracted beams, and l is the diffraction order (an integer).

In the collinear diffraction modulator, β_i, β_d, and k_g are all in the z direction, so that (81) is the condition for most efficient power transfer. Experimentally, exchange of power between two guided modes of a glass waveguide on a quartz substrate has been induced by a collinear traveling acoustic wave [76]. The theoretical treatment of mode coupling by a periodic perturbation in refractive index, which was given in Section III-E, is appropriate to this experimental situation. In a similar experimental arrangement, illustrated in Fig. 11, power was deflected out of a waveguide and into its substrate by a traveling acoustic wave [77]. The theoretical treatment

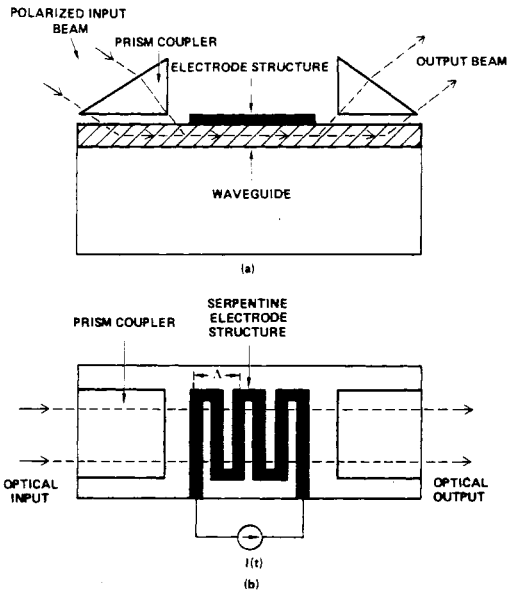

Fig. 10. Magnetooptic thin-film modulator. The serpentine electrode structure produces a spatially periodic modulating field, which rotates the polarization of the guided wave.

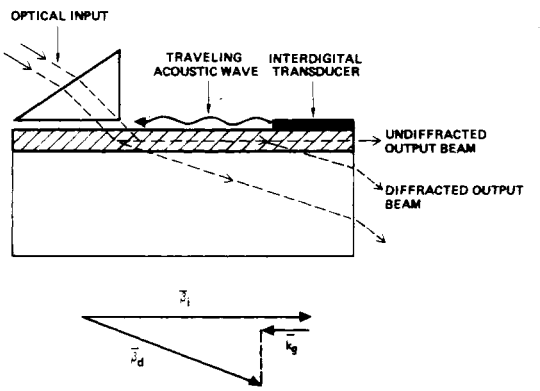

Fig. 11. Collinear acoustooptic modulator, in which an optical beam is diffracted out of the waveguide and into the substrate.

in this case parallels that of guided-to-unguided mode conversion by a grating coupler, given in Section V.

We now consider the more general case in which β_i, β_d, and k_g are not collinear. A sinusoidal perturbation in a diagonal element of the dielectric tensor can be written as

$$\Delta\epsilon_y = \frac{\epsilon_0 \Delta n^2}{2} \left[e^{i[(k_g)_y y + (k_g)_z z]} + e^{-i[(k_g)_y y + (k_g)_z z]} \right]. \quad (82)$$

It is assumed that $\Delta\epsilon_y$ does not vary in the x direction, a reasonable approximation for most of the noncollinear device configurations which have been reported. Based on this assumption, orthogonality of planar waveguide modes requires that the exchange of power between incident and diffracted waves involve modes of the same order. If just one diffracted wave is present, then

$$E_y = e^{i\omega t} \mathcal{E}_y^{(i)}(x) \left[B e^{-i[(\beta_i)_y y + (\beta_i)_z z]} + A e^{-i[(\beta_d)_y y + (\beta_d)_z z]} \right] \quad (83)$$

where A and B are the amplitudes of the diffracted and incident waves, and $(\beta_i)_y^2 + (\beta_i)_z^2 = (\beta_d)_y^2 + (\beta_d)_z^2$. Combining this result with (72), (82), and (36) leads to the usual coupled-mode equations (20), where

$$\kappa = \frac{-i\epsilon_0 \mu \omega^2 \Delta n^2}{4\beta_i} \quad (84)$$

$$\Delta = (\beta_d)_z - (\beta_i)_z \pm (k_g)_z. \quad (85)$$

This assumes that the width of the interaction region in the y direction is large, so that (80) is satisfied, with $l = 1$. If the incident beam is nearly normal to k_g, then (80) implies that

$$\sin\theta \cong \frac{|k_g|}{|\beta_i|} \quad (86)$$

where θ is the angle between β_i and β_d.

We find from (24) that the fraction of power transferred from the incident wave to the diffracted wave p_m is

$$p_d = \frac{\sin^2 \left[\frac{1}{2} (4|\kappa|^2 + \Delta^2)^{1/2} L \right]}{1 + \left(\frac{\Delta^2}{4|\kappa|^2} \right)} \quad (87)$$

where L is the interaction length. Maximum coupling occurs for $\Delta = 0$, in which case (87) reduces to

$$p_d \approx \sin^2 \left[\frac{\pi \Delta n L}{\lambda} \right]. \quad (88)$$

For weak interaction (small κ), the power transfer is appreciable only if Δ is small. In this limit, the condition (81) is satisfied, with $l = 1$. This imposes a restriction on the angle ϕ between β_i and the rulings of the grating: $\phi = \theta/2$. The Bragg condition

$$\sin\phi = \frac{|k_g|}{2|\beta_i|} \quad (89)$$

must be satisfied for efficient coupling.

On the other hand, if the interaction is strong (large κ), the power transfer efficiency does not degrade significantly with increasing Δ. This means that the Bragg restriction (89) no longer must be satisfied for efficient coupling, and exchange of power between different diffracted orders, separated in angle by θ, is possible. In this case, the appropriate differential equation is

$$\frac{dA_n}{dz} = \kappa [A_{n-1} + A_{n+1}] \quad (90)$$

where A_n is the amplitude of the nth-order diffracted mode, and $A_0 \equiv B$ is the amplitude of the incident wave. The solution for this case [78], given by (56), was derived in the discussion of coupling between parallel waveguides. This result was first obtained by Raman and Nath [79].

Electrooptic diffraction modulation of the Raman-Nath type has been demonstrated in 150-μm-thick crystals of $LiNbO_3$ [80]-[82]. Bragg modulation has been reported in films of nitrobenzene liquid on glass substrates [83], [84], and in films of ZnO on Al_2O_3 [85]. An experimental setup for electrooptic Bragg deflection is illustrated in Fig. 12. In contrast to the linear electrooptic crystals, the induced index change in the liquids is a quadratic function of the applied field. Deflection of carbon dioxide laser light in GaAs using a single-electrode Schottky barrier configuration has been observed [86]. Finally, an acoustooptic Bragg-diffraction modulator has been fabricated by depositing a glass film on a quartz substrate, as illustrated in Fig. 13 [87].

In the *waveguide cutoff* modulator, the applied field inhibits or enhances waveguiding. In the case of the asymmetric

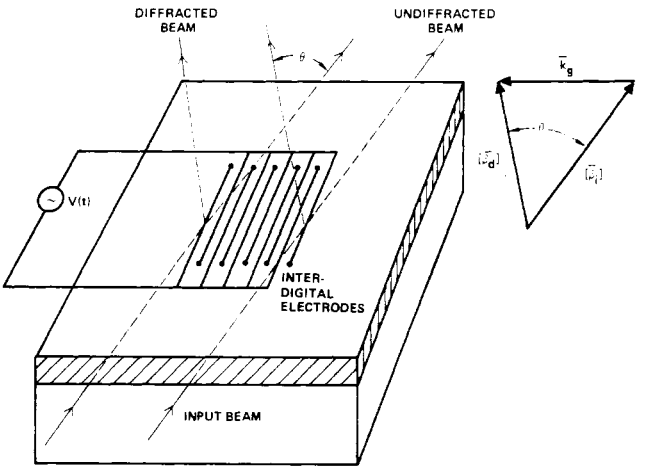

Fig. 12. Electrooptic diffraction modulation in a thin-film waveguide. Voltage applied to the interdigital electrodes causes a periodic variation in refractive index, which deflects part of the guided beam through an angle θ.

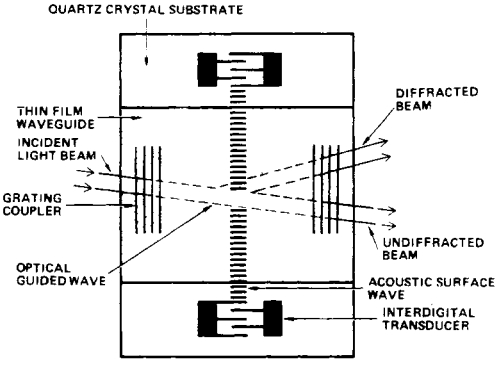

Fig. 13. Acoustooptic thin-film modulator. A surface acoustic wave produces a periodic refractive index variation in the waveguide, which diffracts a guided optical wave.

slab waveguide, illustrated in Fig. 1, in which $n_2 - n_1 \gg n_2 - n_3$, the cutoff condition for both TE and TM modes is approximately given by

$$\sqrt{n_2^2 - n_3^2}\,\frac{t}{\lambda} = \frac{1}{4} \tag{91}$$

where t is the width of the waveguide.

In a planar device in epitaxial layers of GaAs, an applied electric field reduced the waveguide refractive index difference to a value below cutoff [88]. In the presence of the field, the input beam coupled into guided modes and was lost by spreading; with no field, part of the input power was confined by the waveguide. In another experiment, a voltage applied between parallel electrodes on the surface of a bulk $LiNbO_3$ crystal caused a localized increase in refractive index sufficient for waveguiding [89].

Modulation based on *interguide coupling* has not been demonstrated experimentally, but Fig. 14 illustrates how such a device might operate [90]. In the absence of an applied electric field, the waveguides have equal propagation constants, and the length of the coupling region is chosen such that light entering one guide emerges from the other. The applied field causes a reduction in both coupling length and coupling efficiency by destroying the phase matching initially present. A field large enough to reduce the coupling length by a factor of two switches the output to the initially excited guide. According to (53), the appropriate values of κ and Δ for this type of device are $\kappa = \pi/2L$ and $\Delta = \sqrt{3}\pi/L$, where κ is the coupling constant, Δ is the induced difference in propagation constants between the two waveguides, and L is the length of the coupling region. If the refractive index for one waveguide is increased by Δn and that of the other is decreased by the same amount, it follows that $\Delta \approx 4\pi\Delta n/\lambda$, so that

$$\frac{\Delta n L}{\lambda} = \frac{\sqrt{3}}{4}. \tag{92}$$

Attenuation of a guided wave by induced absorption or scattering will modulate its intensity. Mathematically, the attenuation is a result of an imaginary component in diagonal elements of the dielectric tensor. Modulation by scattering has recently been demonstrated in thin-film waveguides of nematic liquid crystals [26], [27]. An applied electric field causes turbulence in the liquid, which becomes less transparent to the guided light wave.

C. Modulator Power Requirements

As mentioned earlier, one of the main reasons that thin-film modulators are of practical interest is that they offer the possibility of low-power operation at wide bandwidths. The external power P_e required for operating a modulator at a bandwidth B is given approximately by

$$P_e = BW \tag{93}$$

where W is the power supplied from an external source to switch the device on or off. In the electrooptic case,

$$W = \frac{1}{2}\int \epsilon E_a^2\, dv \tag{94}$$

where E_a is the applied electric field and the volume integral is over all space. The change in refractive index Δn is related to the applied field by

$$\Delta n = \tfrac{1}{2} n^3 r E_a \tag{95}$$

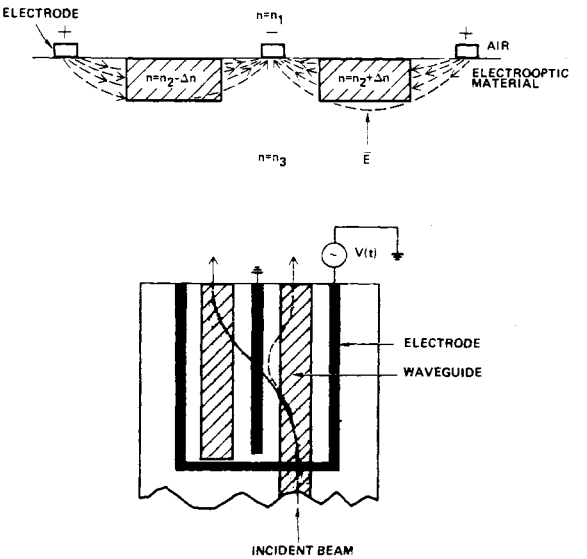

Fig. 14. Proposed electrooptic modulator or switch. (a) The applied field increases the refractive index of one waveguide and decreases that of the other. (b) The applied field causes the coupling length to be shortened, so that the output is transferred from one guide to the other.

where r is the linear electrooptic coefficient. For relative phase, spatial diffraction, and interguide coupling modulators, we have

$$\Delta n L/\lambda \approx \tfrac{1}{2}. \tag{96}$$

From these results, we arrive at the following estimate for the modulation power:

$$P_e \approx \frac{1}{2}\left(\frac{\lambda^2}{n^6 r^2}\right)\left(\frac{wt}{L}\right) B \tag{97}$$

where w and t are the transverse dimensions of the waveguide, and L is the modulation path length. This formula assumes coincidence between the optical guided wave and the applied field.

In the acoustooptic case, the induced index change Δn is related to the acoustic intensity I by an acoustic figure of merit $M = n^6 p^2/\rho V_s^2$, where p is the appropriate photoelastic tensor element, V_s is the acoustic velocity, and ρ is the mass density [91]. The relation is

$$\Delta n = \sqrt{MI/2}. \tag{98}$$

By integrating the expression

$$W = \int I\, dv \tag{99}$$

and recalling (96), we derive the result

$$P_e \approx \frac{1}{2}\left(\frac{\lambda^2}{M}\right)\left(\frac{wt}{L}\right) B. \tag{100}$$

The geometrical factor (wt/L) thus appears in the expressions for both electrooptic and acoustooptic devices, indicating that a reduction in required power can be obtained by minimizing the effective cross-sectional area wt of the device.

Electrical power requirements of only about 0.2 mW/MHz have been reported for two of the planar electrooptic devices: double heterostructure $GaAs\text{-}Al_xGa_{1-x}As$ diodes [70] and $LiNbO_3$ diffused waveguides [71]. This is about two orders of magnitude less than in bulk $LiNbO_3$ modulators [92], and

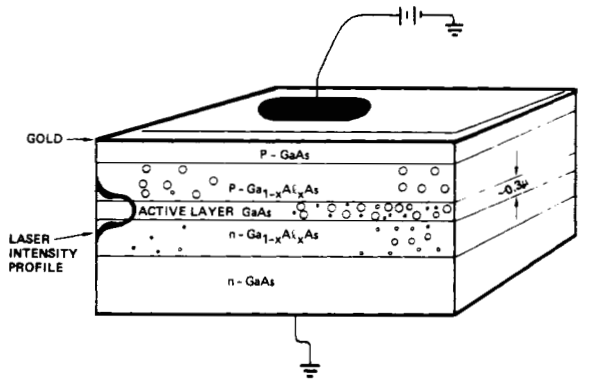

Fig. 15. Schematic diagram of GaAs-$Ga_{1-x}Al_xAs$ injection laser.

a factor of six better than bulk $LiTaO_3$ [93] (which requires close temperature control). Further reduction of power can be anticipated as ways of providing good beam confinement in two dimensions are developed. The recent fabrication of channel waveguides in GaAs-$Al_xGa_{1-x}As$ [40] is encouraging from this standpoint.

VII. Laser Sources

At the present time, the most suitable sources for integrated and guided wave optics are the semiconductor injection lasers. This is due to a number of factors: 1) The basic planar epitaxial fabrication techniques used to make these lasers are very similar to those used to make a large variety of other thin-film waveguide components. 2) The electrical current excitation is compatible for interfacing with conventional electronic circuits. 3) They can be modulated, at least up to the GHz level, by current modulation [94]. 4) The material used most commonly in these lasers, GaAs–GaAlAs, is also an excellent material for fabricating a whole array of other components [95]. It has indeed been used to make thin-film waveguides, modulators, directional couplers, and detectors. This opens the way to the possibility of an integrated optical technology based on a single material, GaAs, and its related alloys, in analogy with the role played by silicon in integrated electronics.

The typical structure [5]–[7] used in fabricating injection lasers is illustrated in Fig. 15. The laser mode is confined in a dielectric waveguide formed by the inner GaAs layer and the $Ga_{1-x}Al_xAs$ layers bounding it which possess a lower index of refraction. Holes injected from the p $Ga_{1-x}Al_xAs$ layer into the inner GaAs layer recombine radiatively with electrons injected from the n $Ga_{1-x}Al_xAs$ layer thus providing the coherent laser radiation. The threshold current intensity decreases with smaller thicknesses of both the optical confinement distance and also of the distance to which the electrons and holes are confined. More recent advances [96], [97] use additional layers for improved electron and optical confinement. Continuous operation with lifetimes of a few thousand hours has been demonstrated [98]. These lifetimes will have to increase by at least an order of magnitude before these diodes can be used in most practical optical systems.

A number of problems still remain to be solved in injection lasers in addition to that of the lifetime. These include the control of the tendancy to oscillate simultaneously in a number of modes and the difficulty of mirror fabrication in laser sources designed to couple monolithically into other components on a single optical chip.

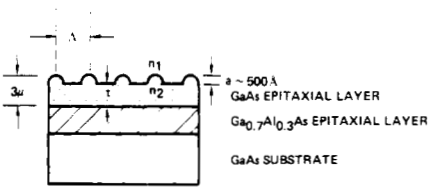

Fig. 16. Corrugated waveguide configuration for distributed feedback laser in GaAs-$Ga_xAl_{1-x}As$.

A recent development which addresses itself to a possible solution to these problems is that of the corrugated waveguide laser [13]. Such a waveguide is illustrated by Fig. 16. The feedback necessary for laser oscillation is provided, not by the conventional end reflectors, but by a series of corrugations separated by half a wavelength which, in a manner equivalent to a multilayer dielectric mirror, reflect a propagating mode, thus coupling the forward and backward modes. The principle involved here, one of distributed feedback, was formulated originally by Kogelnik and Shank [12] and applied by them to dye lasers.

To understand the principle involved in this class of lasers we may go back to the problem of contradirectional coupling considered in Section III. If the coupling between the forward and the backward modes is due to surface corrugations, the coupling coefficient is given by (44).

The coupled-mode equations become

$$\frac{dA}{dz} = \kappa B e^{-i\Delta z} - \alpha A$$

$$\frac{dB}{dz} = \kappa A e^{i\Delta z} + \alpha B \tag{101}$$

where $\Delta = 2\beta - 2\pi/\Lambda$, β is the propagation constant of the unperturbed mode, and Λ is the period of the corrugation. Since here we deal with amplifying media rather than with a passive guide, α is the distributed gain constant.

Assuming a solution of the form

$$A(z) = a(z)\, e^{-i\Delta\beta z}$$

$$B(z) = b(z)\, e^{i\Delta\beta z} \tag{102}$$

where $2\Delta\beta \equiv \Delta$, leads to

$$\frac{da}{dz} = (i\Delta\beta - \alpha)\, a + \kappa b$$

$$\frac{db}{dz} = -(i\Delta\beta - \alpha)\, b + \kappa a. \tag{103}$$

Let us assume for a moment that a wave with amplitude $b(0)$ is incident at $z = 0$ on the corrugated section of length L, as shown in Fig. 5, and we want to find the amplitude ratio $a(0)/b(0)$ of the reflected to incident waves at the input $z = 0$. This expression is obtainable directly from (30), except that, according to (103), we need to replace everywhere $i\Delta/2$ by $i\Delta\beta - \alpha$. The result is thus

$$\frac{a(0)}{b(0)} = \frac{-\kappa \sinh(\gamma L)}{(-\alpha + i\Delta\beta)\sinh(\gamma L) + \gamma \cosh(\gamma L)} \tag{104}$$

$$\gamma^2 \equiv \kappa^2 + (-\alpha + i\Delta\beta)^2. \tag{105}$$

Unlike (30), the ratio $a(0)/b(0)$ can now, for certain values of $\Delta\beta$ and α, go to infinity. This corresponds to a finite reflected

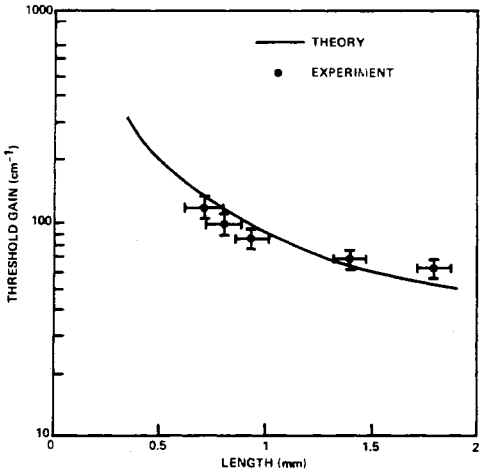

Fig. 17. Theoretical and experimental threshold gain characteristics for a distributed feedback laser in GaAs-$Ga_xAl_{1-x}As$.

wave $a(0)$ with no input $[b(0) = 0]$, i.e., oscillation. The oscillation condition is thus $a(0)/b(0) = \infty$ or, using (104),

$$(-\alpha + i\Delta\beta) = -\gamma \coth(\gamma L) \tag{106}$$

which can also be written as

$$\frac{\gamma + (-\alpha + i\Delta\beta)}{\gamma - (-\alpha + i\Delta\beta)} e^{2\gamma L} = -1. \tag{107}$$

As an example consider the high gain case $\alpha >> \kappa$. Equation (107) can be separated into a set of simultaneous phase and amplitude conditions. The phase condition is

$$2\tan^{-1}\frac{\Delta\beta_m}{\alpha_m} - 2\Delta\beta_m L + \frac{\Delta\beta_m L\kappa^2}{\alpha_m^2 + \Delta\beta_m^2} = (2m+1)\pi,$$
$$m = 0, \pm 1, \pm 2, \cdots. \tag{108}$$

Each value of m in (108) corresponds to a longitudinal mode. In the limit $\alpha >> \Delta\beta$, the modes are given by

$$\Delta\beta_m L = -(m + \tfrac{1}{2})\pi \tag{109}$$

corresponding to frequency intervals between modes

$$\Delta\omega \equiv \omega_m - \omega_{m-1} = \frac{\pi c}{nL} \tag{110}$$

which is the same result as in a Fabry-Perot laser. Note that there is no solution with $\Delta\beta = 0$ which would correspond, according to (101), to the exact Bragg condition $\beta = \pi/\Lambda$.

The threshold gain value α_m of a given mode m is derived by equating the amplitudes on both sides of (107). In the limit $\alpha >> \kappa$, it is

$$\frac{e^{2\alpha_m L}}{\alpha_m^2 + (\Delta\beta_m)^2} = \frac{4}{\kappa^2} \tag{111}$$

indicating an increase in threshold for modes with increasing m. This mode discrimination property of the distributed feedback laser is expected to play an important role in its applications.

Fig. 17 contains experimental data [13] on a laser such as shown in Fig. 16 as well as a theoretical plot of the threshold conditions (111).

VII. Conclusions

The topics covered in the balance of this paper include the main concentration of research to date in guided-wave optical phenomena. However, there have also been several significant contributions which do not fall into the previously discussed categories. These include experimental [65], [99] and theoretical [100]-[102] results on nonlinear interactions in waveguides, experimental demonstration of light amplification [103], and fabrication of waveguide photodetectors [104], [105].

Remarkable progress has clearly been achieved during the past few years in the understanding of guided-wave techniques and phenomena. The extensive research effort has been inspired in large part by a recognized need [16] for thin-film components for use with the new low-loss fibers [106], [107] in wide-band communications. With the extensive technology base that now exists, we can anticipate the emergence in the near future of new devices of considerable practical importance. However, the field is still in its infancy, and we can expect it to be a source of rewarding research topics as well as useful components for years to come.

References

[1] E. Snitzer and H. Osterberg, "Observed dielectric waveguide modes in the visible spectrum," *J. Opt. Soc. Amer.*, vol. 51, pp. 499-505, May 1961.
[2] A. Yariv and R. C. C. Leite, "Dielectric waveguide mode of light propagation in p-n junction," *Appl. Phys. Lett.*, vol. 2, pp. 55-57, Feb. 1, 1963.
[3] W. L. Bond, B. G. Cohen, R. C. C. Leite, and A. Yariv, "Observation of the dielectric waveguide mode of light propagation in p-n junction," *Appl. Phys. Lett.*, vol. 2, pp. 57-59, Feb. 1, 1963.
[4] D. F. Nelson and F. K. Reinhart, "Light modulation by the electrooptic effect in reversed-biased GaP p-n junctions," *Appl. Phys. Lett.*, vol. 5, pp. 148-150, Oct. 1, 1964.
[5] Z. I. Alferov, V. M. Andreev, V. I. Korolkov, E. L. Portnoi, and D. N. Tretyakov, "Coherent radiation of epitaxial heterojunction structures in the AlAs-GaAs system," *Sov. Phys.–Semicond.*, vol. 2, pp. 1289-1291, Apr. 1969.
[6] I. Hayashi, M. B. Panish, and P. W. Foy, "A low-threshold room-temperature injection laser," *IEEE J. Quantum Electron* (Corresp.), vol. QE-5, pp. 211-212, Apr. 1969.
[7] H. Kressel and H. Nelson, "Close-confinement gallium arsenide PN junction lasers with reduced optical loss at room temperature," *RCA Rev.*, vol. 30, pp. 106-113, Mar. 1969.
[8] I. Hayashi, M. B. Panish, P. W. Foy, and S. Sumski, "Junction lasers which operate continuously at room temperature," *Appl. Phys. Lett.*, vol. 17, pp. 109-111, Aug. 1, 1970.
[9] D. Hall, A. Yariv, and E. Garmire, "Optical guiding and electrooptic modulation in GaAs epitaxial layers," *Opt. Commun.*, vol. 1, pp. 403-405, Apr. 1970.
[10] P. K. Tien, R. Ulrich, and R. J. Martin, "Modes of propagating light waves in thin deposited semiconductor films," *Appl. Phys. Lett.*, vol. 14, pp. 291-294, May 1, 1969.
[11] M. L. Dakss, L. Kuhn, P. F. Heidrick, and B. A. Scott, "Grating coupler for efficient excitation of optical guided waves in thin films," *Appl. Phys. Lett.*, vol. 16, pp. 523-525, June 15, 1970.
[12] H. Kogelnik and C. V. Shank, "Coupled-wave theory of distributed feedback lasers," *J. Appl. Phys.*, vol. 43, pp. 2327-2335, May 1972.
[13] M. Nakamura *et al.*, "Laser oscillation in epitaxial GaAs waveguides with corrugation feedback," *Appl. Phys. Lett.*, vol. 23, pp. 224-225, Sept. 1, 1973.
[14] S. Somekh, E. Garmire, A. Yariv, H. L. Garvin, and R. G. Hunsperger, "Channel optical waveguide directional couplers," *Appl. Phys. Lett.*, vol. 22, pp. 46-47, Jan. 15, 1973.
[15] R. Shubert and J. H. Harris, "Optical surface waves on thin films and their application to integrated data processors," *IEEE Trans. Microwave Theory Tech.*, vol. MTT-16, pp. 1048-1054, Dec. 1968.
[16] S. E. Miller, "Integrated optics: An introduction," *Bell Syst. Tech. J.*, vol. 48, pp. 2059-2069, Sept. 1969.
[17] H. Osterberg and L. W. Smith, "Transmission of optical energy

along surfaces: Part II: Inhomogeneous media," *J. Opt. Soc. Amer.*, vol. 58, pp. 1078–1084, Sept. 1964.
[18] D. H. Hensler, J. D. Cuthbert, R. J. Martin, and P. K. Tien, "Optical propagation in sheet and pattern generated films of Ta_2O_5," *Appl. Opt.*, vol. 10, pp. 1037–1042, May 1971.
[19] W. S. C. Chang and K. W. Loh, "Experimental observation of 10.6 μm guided waves in Ge thin films," *Appl. Opt.*, vol. 10, pp. 2361–2362, Oct. 1971.
[20] J. H. Harris, R. Shubert, and J. N. Polky, "Beam coupling to films," *J. Opt. Soc. Amer.*, vol. 60, pp. 1007–1016, Aug. 1970.
[21] P. K. Tien, G. Smolinsky, and R. J. Martin, "Thin organosilicon films for integrated optics," *Appl. Opt.*, vol. 11, pp. 637–642, Mar. 1972.
[22] R. Ulrich, H. P. Weber, E. A. Chandross, W. J. Tomlinson, and E. A. Franke, "Embossed optical waveguides," *Appl. Phys. Lett.*, vol. 20, pp. 213–215, Mar. 15, 1972.
[23] J. C. Dubois, M. Gazard, and D. B. Ostrowsky, "Fabrication of optical waveguides in electron resist films," *Opt. Commun.*, vol. 7, pp. 237–238, Mar. 1973.
[24] T. P. Sosnowski and H. P. Weber, "Thin birefringent polymer films for integrated optics," *Appl. Phys. Lett.*, vol. 21, pp. 310–311, Oct. 1, 1972.
[25] D. P. Gia Russo and J. H. Harris, "Electrooptic modulation in a thin film waveguide," *Appl. Opt.*, vol. 10, pp. 2786–2788, Dec. 1971.
[26] D. J. Channin, "Optical waveguide modulation using nematic liquid crystal," *Appl. Phys. Lett.*, vol. 22, pp. 365–366, Apr. 15, 1973.
[27] J. P. Sheridan, J. M. Schnur, and T. G. Giallorenzi, "Electro-optic switching in low-loss liquid-crystal waveguides," *Appl. Phys. Lett.*, vol. 22, pp. 560–561, June 1, 1973.
[28] J. E. Goell and R. D. Standley, "Sputtered glass waveguide for integrated optical circuits," *Bell Syst. Tech. J.*, vol. 48, pp. 3445–3448, Dec. 1969.
[29] J. E. Goell, "Electron-resist fabrication of bends and couplers for integrated optical circuits," *Appl. Opt.*, vol. 12, pp. 729–736, Apr. 1973.
[30] J. E. Goell, R. D. Standley, W. M. Gibson, and J. W. Rodgers, "Ion bombardment fabrication of optical waveguides using electron resist masks," *Appl. Phys. Lett.*, vol. 21, pp. 72–73, July 15, 1972.
[31] I. P. Kaminow and J. R. Carruthers, "Optical waveguiding layers in $LiNbO_3$ and $LiTaO_3$," *Appl. Phys. Lett.*, vol. 22, pp. 326–328, Apr. 1, 1973.
[32] H. F. Taylor, W. E. Martin, D. B. Hall, and V. N. Smiley, "Fabrication of single-crystal semiconductor optical waveguides by solid-state diffusion," *Appl. Phys. Lett.*, vol. 21, pp. 95–98, Aug. 1, 1972.
[33] W. E. Martin and D. B. Hall, "Optical waveguides by diffusion in II-VI compounds," *Appl. Phys. Lett.*, vol. 21, pp. 325–327, Oct. 1, 1972.
[34] P. K. Cheo, J. M. Berak, W. Oshinsky, and J. L. Swindal, "Optical waveguide structures for CO_2 lasers," *Appl. Opt.*, vol. 12, pp. 500–509, Mar. 1973.
[35] I. Hayashi, M. B. Panish, and F. K. Reinhart, "GaAs–$Al_xGa_{1-x}As$ double heterostructure injection lasers," *J. Appl. Phys.*, vol. 42, pp. 1929–1941, Apr. 1971.
[36] D. Vincent, "Infrared waveguides in silicon," presented at the OSA Topical Meeting on Integrated Optics, Las Vegas, Nev., 1972.
[37] D. B. Hall and C. Yeh, "Leaky waves in a heteroepitaxial film," *J. Appl. Phys.*, vol. 44, pp. 2271–2274, May 1973.
[38] J. M. Hammer, D. J. Channin, M. T. Duffy, and J. P. Wittke, "Low-loss epitaxial ZnO optical waveguides," *Appl. Phys. Lett.*, vol. 21, pp. 358–360, Oct. 15, 1972.
[39] P. K. Tien, R. J. Martin, S. L. Blank, S. H. Wemple, and L. J. Varnerin, "Optical waveguides of single-crystal garnet films," *Appl. Phys. Lett.*, vol. 21, pp. 207–209, Sept. 1, 1972.
[40] J. C. Tracy, W. Wiegman, R. A. Logan, and F. K. Reinhart, "Three-dimensional light guides in single-crystal GaAs–$Al_xGa_{1-x}As$," *Appl. Phys. Lett.*, vol. 22, pp. 511–512, May 15, 1973.
[41] R. A. Logan and F. K. Reinhart, "Optical waveguides in GaAs–AlGaAs epitaxial layers," *J. Appl. Phys.*, vol. 44, pp. 4172–4176, Sept. 1973.
[42] D. Marcuse, *Light Transmission Optics*. New York: Van Nostrand-Reinhold, 1972.
[43] N. S. Kapany and J. J. Burke, *Optical Waveguides*. New York: Academic Press, 1972.
[44] E. A. J. Marcatili, "Dielectric rectangular waveguide and directional coupler for integrated optics," *Bell Syst. Tech. J.*, vol. 48, pp. 2071–2102, Sept. 1969.
[45] J. E. Goell, "A circular-harmonic computer analysis of rectangular dielectric waveguides," *Bell Syst. Tech. J.*, vol. 48, pp. 2133–2160, Sept. 1969.
[46] A. Yariv, "Coupled-mode theory for guided-wave optics," *IEEE J. Quantum Electron.*, vol. QE-9, pp. 919–933, Sept. 1973.
[47] J. R. Pierce, "Coupling of modes of propagation," *J. Appl. Phys.*, vol. 25, pp. 179–183, Feb. 1954.
[48] D. Marcuse, "The coupling of degenerate modes in two parallel dielectric waveguides," *Bell Syst. Tech. J.*, vol. 50, pp. 1791–1816, July-Aug. 1971.
[49] A. L. Jones, "Coupling of optical fibers and scattering in fibers," *J. Opt. Soc. Amer.*, vol. 55, pp. 261–271, Mar. 1965.
[50] H. F. Taylor, "Frequency-selective coupling in parallel dielectric waveguides," *Opt. Commun.*, vol. 8, pp. 421–425, Aug. 1973.
[51] N. S. Kapany, J. J. Burke, K. L. Frame, and R. E. Wilcox, "Coherent interactions between optical waveguides and lasers," *J. Opt. Soc. Amer.*, vol. 58, pp. 1176–1183, Sept. 1968.
[52] A. Ihaya, H. Furuta, and H. Noda, "Thin-film optical directional coupler," *IEEE J. Quantum Electron. (1972 Int. Quantum Electronics Conf.*, Dig. Tech. Papers), vol. QE-8, pp. 546–547, June 1972.
[53] H. L. Garvin, E. Garmire, S. Somekh, H. Stoll, and A. Yariv, "Ion beam micromachining of integrated optics components," *Appl. Opt.*, vol. 12, pp. 455–459, Mar. 1973.
[54] C. Elachi and C. Yeh, "Frequency selective coupler for integrated optics systems," *Opt. Commun.*, vol. 7, pp. 201–204, Mar. 1973.
[55] L. V. Iogansen, "Theory of resonant electromagnetic systems with total internal reflection," *Sov. Phys.–Tech. Phys.*, vol. 11, pp. 1529–1534, May 1967.
[56] R. Ulrich, "Optimum excitation of optical surface waves," *J. Opt. Soc. Amer.*, vol. 61, pp. 1467–1477, Nov. 1971.
[57] J. H. Harris, R. K. Winn, and D. G. Dalgoutte, "Theory and design of periodic couplers," *Appl. Opt.*, vol. 11, pp. 2234–2241, Oct. 1972.
[58] M. Neviere, R. Petit, and M. Cadilhac, "About the theory of optical grating coupler-waveguide systems," *Opt. Commun.*, vol. 8, pp. 113–117, June 1973.
[59] K. Ogawa and W. S. C. Chang, "Analysis of holographic thin film grating coupler," *Appl. Opt.*, vol. 12, pp. 2167–2171, Sept. 1973.
[60] S. T. Peng, T. Tamir, and H. L. Bertoni, "Leaky-wave analysis of optical periodic couplers," *Electron. Lett.*, vol. 9, pp. 150–152, Mar 22, 1973.
[61] H. Kogelnik and T. P. Sosnowski, "Holographic thin film couplers," *Bell Syst. Tech. J.*, vol. 49, pp. 1602–1608, Sept. 1970.
[62] D. G. Dalgoutte, "A high efficiency thin grating coupler for integrated optics," *Opt. Commun.*, vol. 8, pp. 124–127, June 1973.
[63] P. K. Tien and R. J. Martin, "Experiments of light waves in a thin tapered film and a new light-wave coupler," *Appl. Phys. Lett.*, vol. 18, pp. 398–401, May 1, 1971.
[64] J. H. Harris and R. Shubert, "Variable tunneling excitation of optical surface waves," *IEEE Trans. Microwave Theory Tech.*, vol. MTT-19, pp. 269–276, Mar. 1971.
[65] P. K. Tien, "Light waves in thin films and integrated optics," *Appl. Opt.*, vol. 10, pp. 2395–2413, Nov. 1971.
[66] K. Ogawa, W. S. C. Chang, B. L. Sopori, and F. J. Rosenbaum, "A theoretical analysis of etched grating couplers for integrated optics," *IEEE J. Quantum Electron.*, vol. QE-9, pt. I, pp. 29–42, Jan. 1973.
[67] I. P. Kaminow and E. H. Turner, "Electrooptic light modulators," *Proc. IEEE*, vol. 54, pp. 1374–1390, Oct. 1966.
[68] F. K. Reinhart, "Reverse-biased gallium phosphide diodes as high-frequency light modulators," *J. Appl. Phys.*, vol. 39, pp. 3426–3434, June 1968.
[69] F. K. Reinhart, D. F. Nelson, and J. McKenna, "Electro-optic and waveguide properties of reverse-biased gallium phosphide pn junctions," *Phys. Rev.*, vol. 177, pp. 1208–1221, Jan. 15, 1969.
[70] F. K. Reinhart and B. I. Miller, "Efficient GaAs–$Al_xGa_{1-x}As$ double heterostructure light modulators," *Appl. Phys. Lett.*, vol. 20, pp. 36–38, Jan. 1, 1972.
[71] I. P. Kaminow, J. R. Carruthers, E. H. Turner, and J. W. Stulz, "Thin-film $LiNbO_3$ electro-optic light modulator," *Appl. Phys. Lett.*, vol. 22, pp. 540–542, May 15, 1973.
[72] W. E. Martin, "Waveguide electro-optic modulation in II-VI compounds," *J. Appl. Phys.*, vol. 44, pp. 3703–3707, Aug. 1973.
[73] P. K. Tien, R. J. Martin, R. Wolfe, R. C. LeCraw, and S. L. Blank, "Switching and modulation of light in magneto-optic waveguides of garnet films," *Appl. Phys. Lett.*, vol. 21, pp. 394–396, Oct. 15, 1972.
[74] M. L. Shah, "Fast acousto-optical waveguide modulators," *Appl. Phys. Lett.*, vol. 23, pp. 75–77, July 15, 1973.
[75] G. B. Brandt, M. Gottlieb, and J. J. Conroy, "Bulk acoustic wave interaction with guided optical waves," *Appl. Phys. Lett.*,

vol. 23, pp. 53–54, July 15, 1973.
[76] L. Kuhn, P. F. Heidrich, and E. G. Lean, "Optical guided wave mode conversion by an acoustic surface wave," *Appl. Phys. Lett.*, vol. 19, pp. 428–430, Nov. 15, 1971.
[77] F. R. Gfeller and C. W. Pitt, "Colinear acousto-optic deflection in thin films," *Electron. Lett.*, vol. 8, pp. 549–551, Nov. 2, 1972.
[78] W. R. Klein and B. D. Cook, "Unified approach to ultrasonic light diffraction," *IEEE Trans. Sonics Ultrason.*, vol. SU-14, pp. 123–134, July 1967.
[79] C. V. Raman and N. S. N. Nath, "The diffraction of light by sound waves of high frequency: Pt. II," *Proc. Indian Acad. Sci.*, vol. 2, pp. 413–420, Oct. 1935.
[80] J. M. Hammer, "Digital electrooptic grating deflector and modulator," *Appl. Phys. Lett.*, vol. 18, pp. 147–149, Feb. 15, 1971.
[81] M. A. R. P. de Barros and M. G. F. Wilson, "High-speed electrooptic diffraction modulator for baseband operation," *Proc. Inst. Elec. Eng.*, vol. 119, pp. 807–814, July 1972.
[82] S. Wright and M. G. F. Wilson, "New form of electro-optic deflector," *Electron. Lett.*, vol. 9, pp. 169–170, May 3, 1973.
[83] D. P. Gia Russo and J. H. Harris, "Electrooptic modulation in a thin film waveguide," *Appl. Opt.*, vol. 10, pp. 2786–2788, Dec. 1971.
[84] J. N. Polky and J. H. Harris, "Interdigital electrooptic thin-film modulator," *Appl. Phys. Lett.*, vol. 21, pp. 307–309, Oct. 1, 1972.
[85] J. M. Hammer, D. J. Channin, and M. T. Duffy, "Fast electro-optic waveguide deflector modulator," *Appl. Phys. Lett.*, vol. 23, pp. 176–177, Aug. 15, 1973.
[86] P. K. Cheo, "Pulse amplitude modulation of a CO_2 laser in an electro-optic thin-film waveguide," *Appl. Phys. Lett.*, vol. 22, pp. 241–244, Mar. 1, 1973.
[87] L. Kuhn, M. L. Dakss, P. F. Heidrich, and B. A. Scott, "Deflection of an optical guided wave by a surface acoustic wave," *Appl. Phys. Lett.*, vol. 17, pp. 265–267, Sept. 15, 1970.
[88] D. Hall, A. Yariv, and E. Garmire, "Observation of propagation cutoff and its control in thin optical waveguides," *Appl. Phys. Lett.*, vol. 17, pp. 127–129, Aug. 1, 1970.
[89] D. J. Channin, "Voltage-induced optical waveguide," *Appl. Phys. Lett.*, vol. 19, pp. 128–130, Sept. 1, 1971.
[90] H. F. Taylor, "Optical switching and modulation in parallel dielectric waveguides," *J. Appl. Phys.*, vol. 44, pp. 3257–3262, July 1973.
[91] R. W. Dixon, "Photoelastic properties of selected materials and their relevance for applications to acoustic light modulators and scanners," *J. Appl. Phys.*, vol. 38, pp. 5149–5153, Dec. 1967.
[92] K. K. Chow, R. L. Comstock, and W. B. Leonard, "1.5-GHz bandwidth light modulator," *IEEE J. Quantum Electron.* (Corresp.), vol. QE-5, pp. 618–620, Dec. 1969.
[93] R. T. Denton, F. S. Chen, and A. A. Ballman, "Lithium tantalate light modulators," *J. Appl. Phys.*, vol. 38, pp. 1611–1617, Mar. 15, 1967.
[94] M. Chown, A. R. Goodwin, D. F. Lovelace, G. H. B. Thompson, and P. R. Selway, "Direct modulation of double-heterostructure lasers at rates up to 1 Gbit/s," *Electron. Lett.*, vol. 9, pp. 34–36, Jan. 25, 1973.
[95] A. Yariv, "Components for integrated optics," *Laser Focus*, vol. 8, pp. 40–42, Dec. 1972.
[96] G. H. B. Thompson and P. A. Kirkby, "(GaAl)As lasers with a heterostructure for optical confinement and additional heterojunctions for extreme carrier confinement," *IEEE J. Quantum Electron.*, vol QE-9, pt. II, pp. 311–318, Feb. 1973.
[97] M. B. Panish, H. C. Casey, S. Sumski, and P. W. Foy, "Reduction of threshold current density in GaAs-$Al_xGa_{1-x}As$ heterostructure lasers by separate optical and carrier confinement," *Appl. Phys. Lett.*, vol. 22, pp. 590–591, June 1, 1973.
[98] R. L. Hartman, J. C. Dyment, C. J. Hwang, and M. Kuhn, "Continuous operation of GaAs-$Ga_{1-x}Al_xAs$ double-heterostructure lasers with 30°C half-lives exceeding 1000 h," *Appl. Phys. Lett.*, vol. 23, pp. 181–183, Aug. 15, 1973.
[99] D. B. Anderson and J. T. Boyd, "Wideband CO_2 laser second harmonic generation phase matched in GaAs thin-film waveguides," *Appl. Phys. Lett.*, vol. 19, pp. 266–268, Oct. 15, 1971.
[100] R. A. Andrews, "Crystal symmetry effects on nonlinear optical processes in optical waveguide," *IEEE J. Quantum Electron.*, vol. QE-7, pp. 523–529, Nov. 1971.
[101] S. Somekh and A. Yariv, "Phase-matchable nonlinear optical interactions in periodic thin films," *Appl. Phys. Lett.*, vol. 21, pp. 140–141, Aug. 15, 1972.
[102] W. K. Burns and R. A. Andrews, "Noncritical phase matching in optical waveguides," *Appl. Phys. Lett.*, vol. 22, pp. 143–145, Feb. 15, 1973.
[103] M. S. Chang, P. Burlamacchi, C. Hu, and J. R. Whinnery, "Light amplification in a thin film," *Appl. Phys. Lett.*, vol. 20, pp. 313–314, Apr. 15, 1972.
[104] D. B. Ostrowsky, R. Poirier, L. M. Reiber, and C. Deverdun, "Integrated optical photodetector," *Appl. Phys. Lett.*, vol. 22, pp. 463–464, May 1, 1973.
[105] H. Stoll, A. Yariv, R. G. Hunsperger, and G. L. Tangonan, "Proton implanted optical waveguide detectors in GaAs," *Appl. Phys. Lett.*, vol. 23, pp. 664–665, Dec. 15, 1973.
[106] R. D. Maurer, "Glass fibers for optical communications," *Proc. IEEE*, vol. 61, pp. 452–462, Apr. 1973.
[107] S. E. Miller, E. A. J. Marcatili, and T. Li, "Research toward optical-fiber transmission systems. Part I: The transmission medium," *Proc. IEEE*, vol. 61, pp. 1703–1726, Dec. 1973.
S. E. Miller, T. Li, and E. A. J. Marcatili, "Research toward optical-fiber transmission systems. Part II: Devices and systems considerations," *Proc. IEEE*, vol. 61, pp. 1726–1751, Dec. 1973.